Metasomatic zoning: Appearance of ghost zones in the limit of pure advective mass transport

Article *in* Geochimica et Cosmochimica Acta · January 1993

DOI: 10.1016/0016-7037(93)90438-3

CITATIONS
13

READS
50

2 authors:

Peter Lichtner
University of New Mexico
231 PUBLICATIONS **7,140** CITATIONS
SEE PROFILE

Victor N. Balashov
Pennsylvania State University
73 PUBLICATIONS **641** CITATIONS
SEE PROFILE

Geochimica et Cosmochimica Acta Vol. 57, pp. 369–387

0016-7037/93/$5.00 + .00

Metasomatic zoning: Appearance of ghost zones in the limit of pure advective mass transport

PETER C. LICHTNER[1,*] and VICTOR N. BALASHOV[2]

[1]Hydrochemie, Gruppe, Geologisches und Mineralogisch-petrographisches Institut, Universität Bern, Baltzer-Strasse 1, CH-3012 Bern, Switzerland

[2]Institute of Experimental Mineralogy, 142432 Chernogolovka, Moskow District, Russia

(*Received June* 24, 1991; *accepted in revised form July* 22, 1992)

Abstract—The properties of mineral reaction zones which propagate without changing shape are investigated for a hypothetical two-component system involving advective and diffusive transport in a porous medium. Given sufficient time the width of such zones, referred to as ghost zones, is constant and proportional to the characteristic diffusion or dispersion length of the system. The proportionality factor depends only on the equilibrium constants of the reacting minerals and on the composition of the inlet fluid. As the fluid velocity increases the width of the ghost zone decreases in the case of diffusive transport, and remains constant for dispersive transport for a dispersion coefficient proportional to the fluid velocity. This behavior is contrary to that of normal reaction zones which increase in width in proportion to the fluid velocity. For pure advective transport under conditions of local chemical equilibrium, a ghost zone has zero width. Nevertheless, minerals contained in the ghost zone buffer the downstream fluid composition in spite of their material absence, whence the term *ghost*. By taking into account transport by diffusion or dispersion, the width of a ghost zone has a finite, non-zero value with a well-defined modal composition. In a surface controlled representation of mineral reaction rates for pure advective transport, the width of the ghost zone is finite, but tends towards zero as the kinetic rate constant approaches infinity.

LIST OF SYMBOLS

$\mathcal{A}_j$	designation for the jth primary species.
$\mathcal{A}_i$	designation for the ith aqueous complex.
a_k	concentration of species A within the $k+1$st reaction zone [mol L^{-1}].
b_k	concentration of species B within the $k+1$st reaction zone [mol L^{-1}].
C_i^k	concentration of the ith reversibly reacting aqueous complex within the kth reaction zone [mol L^{-1}].
C_j^k	concentration of the jth primary species within the kth reaction zone [mol L^{-1}].
$C_j^{(k\pm)}$	concentration of the jth primary species evaluated from the left $\langle k+\rangle$ and right $\langle -\rangle$ of the kth reaction zone boundary [mol L^{-1}].
C_j^0	inlet concentration of the jth species [mol L^{-1}].
C_j^∞	initial concentration of the jth species [mol L^{-1}].
D	diffusion coefficient [$cm^2\ s^{-1}$].
I_m^k	reaction rate of the mth mineral within the kth reaction zone [mol $cm^{-3}_{bulk\ vol.}\ s^{-1}$].
J_j^k	solute flux of the jth primary species within the kth reaction zone [mol $cm^{-2}\ s^{-1}$].
K_m	equilibrium constant corresponding to the mth mineral [dimensionless].
$\hat{\mathcal{L}}$	differential operator [s^{-1}].
$l_k(t)$	position of the kth reaction front [cm].
$\mathcal{M}_m$	designation for the mth mineral.
M	number of reacting minerals.
N	number of primary species.
S_m^k	concentration of the mth mineral in the kth reaction zone [mol $cm^{-3}_{bulk\ vol.}$]
t, t'	time coordinates [s].
u	Darcy fluid velocity [cm s^{-1}].
$\bar{V}_m$	molar volume of the mth mineral [$cm^3\ mol^{-1}$].
v	average fluid velocity [cm s^{-1}].
v_k	velocity of the kth reaction front [cm s^{-1}].
x, x'	spatial coordinates [cm].
γ_j	aqueous activity coefficients for the jth species.
Δl	width of ghost zone in asymptotic limit [cm].
Δl_k	width of kth reaction zone [cm].
Δt	time step.
$\delta(x)$	Dirac delta function [cm^{-1}].
η	similarity variable [dimensionless].
η_k	similarity variable for the kth reaction front [dimensionless].
λ	characteristic diffusion length [cm].
ν_{ji}^{aq}	stoichiometric reaction matrix for reversibly reacting aqueous complexes.
ν_{jm}	stoichiometric reaction matrix for mineral reactions.
τ_k	time at which the downstream boundary of the kth reaction zone coincides with the observation point x [s].
ϕ	porosity [dimensionless].
ϕ_m	volume fraction of the mth mineral [dimensionless].
ϕ_m^∞	initial volume fraction of the mth mineral [dimensionless].
χ_α	concentration of conserved quantity [mol L^{-1}].
χ_{AB}	difference of solute concentrations A and B [mol L^{-1}].
Ψ_j	generalized concentration of the jth primary species [mol L^{-1}].
Ψ_j^0	generalized inlet concentration of the jth primary species [mol L^{-1}].
Ψ_j^∞	generalized initial concentration of the jth primary species [mol L^{-1}].
Ω_j	generalized flux of the jth primary species.
$[\cdots]_k$	designating the jump in the enclosed quantity . . . across the kth reaction front.
$\langle k\pm\rangle$	superscript to denote the upstream $\langle +\rangle$ and downstream $\langle -\rangle$ sides of the kth reaction front.

INTRODUCTION

THE APPLICATION OF MASS transport equations to describe quantitatively geochemical systems involving advective and diffusive transport is a rapidly growing field of endeavor (LASAGA, 1984; WALSH et al., 1984; BALASHOV, 1985; LICHTNER, 1985; MERINO et al., 1986; SCHECHTER et al., 1987; LICHTNER, 1988; NOVAK et al., 1989; STEEFEL and VAN CAPPELLEN, 1990; BALASHOV and LEBEDEVA, 1991; LICHTNER, 1992a,b; LICHTNER and BIINO, 1992; LICHTNER and WABER, 1992). The transport equations are based on the simple, yet fundamental, principle of conservation of mass. However, many details of the actual physical system are neglected by averaging over a representative elemental volume (REV) of the porous medium. In this

* *Present address:* Center for Nuclear Waste Regulatory Analysis, Southwest Research Institute, San Antonio, TX 78228-0510, USA.

formulation a real system is approximated by a set of interacting continua which represents, no doubt, a significant simplification of most natural systems. Therefore, when applying these equations to a real system it is important to fully understand, from a general point of view, the basic properties of solutions to the governing mass transport equations. For example, it is now well established that one-dimensional, scalable solutions to kinetic mass transport equations depend only weakly, for sufficiently long time spans, on the choice of kinetic rate constants (LICHTNER, 1988, 1991, 1992a). The purpose of this paper is to explore yet another basic property of solutions to the one-dimensional transport equations, that of the occurrence of so-called ghost zones, or mineral alteration zones which propagate with constant width.

Metasomatic zoning of a host rock resulting from infiltration of fluid in disequilibrium with minerals contained in the rock is a commonly observed phenomena in many geochemical systems. According to the mass transport equations, the width of alteration zones generally increases with increasing time in proportion to the fluid velocity. Recently, however, SCHECHTER et al. (1987) have pointed out the existence of solutions to the transport equations which describe reaction zones which propagate with constant width, rather than increasing in width as do normal zones. In the present work these zones are called ghost zones (BALASHOV and LICHTNER, 1991). The term "ghost zone" is derived from the property that the width of such a zone vanishes in the mathematical limit of pure advective transport and for conditions of local equilibrium and yet, in spite of its material absence, minerals in the zone still buffer the downstream solution composition.

The purpose of this work is to investigate the properties of ghost zones for a simple two-component system with transport by advection and diffusion in a homogeneous porous medium. KORZHINSKII (1970) was perhaps the first to recognize that for pure advection certain zones must disappear that normally would be expected to occur in the sequence of reaction zones. He pointed out that by including diffusion all possible zones appear, but he did not recognize the existence of ghost zones. By continuity of the solution to the mass transport equations in the limit as the diffusion coefficient becomes vanishingly small, it is to be expected that a pure advective solution should necessarily exist. However, the nature of the limiting solution containing zones of zero width comes as a surprise. It must be emphasized that in real systems, in which diffusion or dispersion is always present, ghost zones should be observable, if they exist, possessing a finite width. Although these zones have yet to be identified in natural systems, they may play an important role in weathering, ore genesis, and other processes of geologic importance. A discovery of ghost zones in natural systems would lend strong support for further application of these equations towards investigating metasomatic zoning. The main purpose of this paper, however, is not to address the existence of ghost zones in natural systems, but rather to point out their mathematical existence in solutions to the mass transport equations and to explore some of their properties.

TWO-COMPONENT SYSTEM

The basic problem in a quantitative description of metasomatic zoning is to determine the sequence of reaction zones which form the spatial and time dependence of the solute concentrations and mineral modal abundances within each zone, and the velocities of the zone boundaries. Mathematically this defines a moving boundary problem. The quantities of interest are obtained as solutions to a set of partial differential equations representing conservation of mass for transport and chemical reaction of solute species with minerals. The solution to the transport equations is completely determined for given initial and boundary conditions. These are specified by the initial modal composition of the unaltered host rock, the initial fluid composition in contact with the minerals in the rock, and either the fluid composition or fluid flux entering the column of rock at one end.

Consider a two-component system described by hypothetical species A and B which form minerals A_2B, AB, and AB_2 according to the chemical reactions

$$A + 2B \rightleftharpoons AB_2, \tag{1}$$

$$A + B \rightleftharpoons AB, \tag{2}$$

and

$$2A + B \rightleftharpoons A_2B. \tag{3}$$

Fluid infiltrating into a porous column of rock containing one or more of these minerals produces a sequence of reaction zones which propagate with time. For conditions of local chemical equilibrium, the restriction to a two-component system greatly simplifies the problem. In this case the solute concentration downstream from a reaction front separating two monomineralic zones forms an invariant point determined by mineral equilibria alone. Within this system a number of distinct alteration zone sequences are possible. Consider a host rock consisting initially of mineral A_2B. Any of the reaction zone sequences shown in Fig. 1 are possible. Which sequence actually occurs depends on the composition of the infiltrating fluid at the inlet to the porous rock column, the equilibrium constants of the reacting minerals, modal composition of the host rock, and whether transport occurs by advection, diffusion, or both. Furthermore, the zone sequence may change with time. For cases II, III, and IV the velocities of the zone boundaries are in increasing order consistent with the mineral sequence. The reaction zones grow continuously with time in proportion to the fluid velocity.

POSSIBLE ZONE SEQUENCES

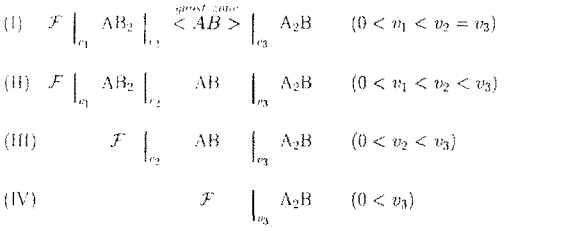

FIG. 1. Several possible mineral zone sequences for a two-component system with the initial host rock consisting of mineral A_2B. Case (I) corresponds to AB as ghost zone, whereas cases II, III, and IV correspond to normal zone sequences. When diffusion is included in the description the zone sequence may change with time. Not all possible zone sequences are shown.

For case I the velocity of the upstream boundary of zone AB is equal to the velocity of its downstream boundary. In this case zone AB is trapped between zones AB_2 and A_2B, and its width has a constant value. The zone AB is referred to as a ghost zone for reasons which become apparent from the following text.

Within the kth reaction zone containing the mth mineral, mass transport equations for solute species A and B for combined advection and diffusion can be expressed in the form (LICHTNER, 1985):

$$\frac{\partial \phi C_j^{(k)}}{\partial t} + \nu_{jm} \frac{\partial S_m^{(k)}}{\partial t} + \frac{\partial J_j^{(k)}}{\partial x} = 0, \tag{4}$$

for j = A, B. In this equation t denotes the time and x the distance measured from the inlet to the porous column of rock, $C_j^{(k)}$ denotes the concentration of the jth solute species, and $J_j^{(k)}$ denotes the solute flux defined by

$$J_j^{(k)} = -\phi D \frac{\partial C_j^{(k)}}{\partial x} + u C_j^{(k)}, \tag{5}$$

where D denotes the diffusion coefficient and u the Darcy flow velocity. The quantity $S_m^{(k)}$ denotes the concentration of the mth mineral defined in terms of the mineral volume fraction ϕ_m by the expression

$$S_m = \bar{V}_m^{-1} \phi_m, \tag{6}$$

where $\bar{V}_m$ denotes the mineral molar volume. The stoichiometric coefficients ν_{jm} refer to the mineral reactions as written in Eqns. 1, 2, and 3. For conditions of local chemical equilibrium the transport equations are solved subject to algebraic constraints corresponding to the mass action equations of the reacting minerals in each zone, which may be expressed in the general form

$$K_m C_A^{\nu_{Am}} C_B^{\nu_{Bm}} = 1. \tag{7}$$

The mass transport equations together with the mineral mass action constraints provide an equal number of equations as unknowns.

It is assumed that initially at $t = 0$, mineral A_2B is the only mineral present in the porous column with abundance $S^0_{A_2B}$. The aqueous solution in equilibrium with the unaltered host rock has the composition

$$C_j(x, 0) = C_j^{\infty}. \tag{8}$$

An aqueous solution undersaturated with respect to minerals AB_2, AB and A_2B with composition

$$C_j(0, t) = C_j^0, \tag{9}$$

enters the porous column at $x = 0$. To simplify the problem the initial solution in contact with mineral A_2B is assumed also to be in equilibrium with mineral AB, thus forming an invariant composition. This condition eliminates internal reaction within the zone occupied by mineral A_2B in the case of diffusive transport. For the other zones, however, internal reaction generally does occur as discussed in Appendix A.

Pure Advective Transport: Definition of Ghost Zone

A description of fluid transport by pure advection in a porous medium in which diffusion is absent, combined with chemical reactions involving minerals and aqueous species, provides a simple algorithm by which metasomatic zoning of a host rock can be calculated. This formulation represents a highly idealized description of natural systems in which diffusion is always present. However, in many instances, diffusion is only important during the initial stages of the time development of a system and can be safely ignored as time goes on (LICHTNER, 1992a). The case of pure advective transport has been analyzed in great detail in the literature (WALSH et al., 1984; LICHTNER, 1991), and only a brief outline is given here with emphasis on the conditions necessary for mineral AB to occur as a ghost zone.

As an advecting fluid infiltrates into a porous column of rock consisting of the single mineral A_2B, a sequence of reaction zones is formed as depicted schematically in Fig. 2 for the zone sequence $\mathcal{F}|AB_2|AB|A_2B$. The first zone denoted by $\mathcal{F}$ corresponds to pure fluid in which all minerals have completely dissolved. The fourth zone is the unaltered host rock, in this case represented by mineral A_2B. The quantity l_0 refers to the inlet to the porous column of rock. In certain circumstances the velocities of zone boundaries l_2 and l_3 may be equal. In this case zone AB is referred to as a ghost zone for reasons given below. To investigate this situation the discussion that follows is restricted to a two-component system. For conditions of local chemical equilibrium this greatly simplifies the problem since, with the exception of the first zone containing mineral AB_2, the solute concentration at reaction fronts l_2 and l_3 form invariant points, determined by mineral equilibria alone. This neglects the variation in mineral equilibrium constants with pressure, of no consequence in this work.

Characteristic of pure advective transport and local equilibrium of minerals is the occurrence of chemical shock fronts across the boundaries of mineral alteration zones. A chemical shock front represents a discontinuous change in the solute concentration at a point in space separating two distinct mineral assemblages. The shock propagates with time in response to the flow of fluid. The velocity of propagation of the shock is determined by conservation of mass across the shock front. These equations relate the velocity of the front to jump discontinuities in the solute flux and mineral modal abundances across the front. The reaction fronts propagate

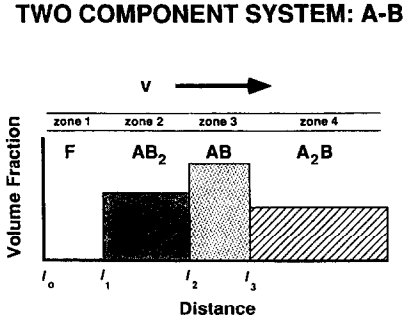

FIG. 2. Schematic illustration of reaction zones in the two-component system A-B for pure advective transport under conditions of local equilibrium. Reaction fronts l_2 and l_3 are invariant points, the fluid composition fixed by equilibrium with minerals AB_2 and AB, and AB and A_2B, respectively. Zone AB is referred to as a ghost zone when $v_2 = v_3$.

with velocities determined by conservation of mass across each front. These equations relate the front velocity to jump discontinuities in the flux and mineral volume fraction, according to (LICHTNER, 1985, 1991):

$$v_k = \frac{dl_k}{dt} = \frac{[J_j]_k}{[\phi C_j]_k + \sum_m \nu_{jm}[S_m]_k}, \tag{10}$$

for the kth reaction front, with j = A, B and m = AB_2, AB, A_2B. Square brackets $[\cdots]_k$ surrounding some quantity denote the jump in the enclosed quantity across the kth front:

$$[f]_k = f^{\langle k+\rangle} - f^{\langle k-\rangle}, \tag{11}$$

where the superscripts $\langle k\pm\rangle$ enclosed in angular brackets signify that f is evaluated on the right $\langle k+\rangle$, or downstream side, and left $\langle k-\rangle$, or upstream side of the kth front. These equations are referred to as the generalized Rankine-Hugoniot equations because of their resemblance to the equations describing the propagation of a shock wave (LICHTNER, 1985, 1991). Note that each solute species which takes part in chemical reactions across the kth front leads to the same velocity v_k, and thus each front represents a coherent wave.

For pure advective transport with mineral reactions governed by local chemical equilibrium, the mass conservation equations are given by

$$\frac{\partial}{\partial t}(\phi C_j) + \frac{\partial J_j}{\partial x} = -\sum_m \nu_{jm} I_m, \tag{12}$$

where the solute flux J_j is given by

$$J_j = uC_j, \tag{13}$$

and where I_m denotes the reaction rate of the mth mineral with stoichiometric reaction coefficient ν_{jm}. For conditions of local equilibrium, the reaction rate is localized at each reaction front proportional to a δ-function singularity according to the expression (LICHTNER, 1991):

$$I_m^k = -v_k \bar{V}_m^{-1}[\phi_m]_k \delta(x - l_k(t)), \tag{14}$$

corresponding to the kth reaction front with m = AB_2, AB, A_2B, where v_k denotes the velocity of the kth front with position l_k. The minus sign ensures that the replacement front l_k moves in the direction of fluid transport. To complete these equations it is necessary to combine them with the appropriate mass action equations as discussed in the following text. The pure advective problem is solved without the need to explicitly consider the rates of reaction of the various minerals at reaction fronts. The reaction rate at zone boundaries is a mathematically singular quantity described by distribution theory, proportional to the Dirac delta function (LICHTNER, 1985, 1991). This singular rate gives rise to an instantaneous nonzero value for the modal abundance of each alteration mineral at its contact with the downstream zone describing the replacement of one mineral by another. The instantaneous value of the mineral modal abundance resulting from replacement reactions at zone boundaries is determined by conservation of mass across the front.

In the following analysis, the Darcy velocity u is assumed constant throughout the porous rock column. For pure advective transport, the concentration itself is discontinuous across each reaction front for those solute species which are involved in mineral reactions on either side of the front, with the jump in flux given by the expression

$$[J_j]_k = u[C_j]_k. \tag{15}$$

According to the previous notation, this equation may be expressed according to

$$[J_j]_k = u(C_j^{\langle k+\rangle} - C_j^{\langle k-\rangle}). \tag{16}$$

The mass transport equations reduce to a set of algebraic equations representing conservation of mass across each reaction front. Within each reaction zone the solute concentration and mineral modal abundance are constant. Applying Eqn. 10 to the reaction zone sequence $\mathcal{F}\,|\,AB_2\,|\,AB\,|\,A_2B$ leads to the equations

$$v_1 = u\frac{a_1 - a_0}{(\phi_1 a_1 - \phi_0 a_0) + S_{AB_2}} = u\frac{b_1 - b_0}{(\phi_1 b_1 - \phi_0 b_0) + 2S_{AB_2}}, \tag{17}$$

$$v_2 = u\frac{a_2 - a_1}{(\phi_2 a_2 - \phi_1 a_1) + S_{AB} - S_{AB_2}} = u\frac{b_2 - b_1}{(\phi_2 b_2 - \phi_1 b_1) + S_{AB} - 2S_{AB_2}}, \tag{18}$$

and

$$v_3 = u\frac{a_3 - a_2}{(\phi_3 a_3 - \phi_2 a_2) + 2S^0_{A_2B} - S_{AB}} = u\frac{b_3 - b_2}{(\phi_3 b_3 - \phi_2 b_2) + S^0_{A_2B} - S_{AB}}, \tag{19}$$

relating the front velocities v_1, v_2, and v_3 to jump discontinuities in the solute concentration and mineral volume fraction across each front. In these equations the initial concentration of mineral A_2B is denoted by $S^0_{A_2B}$, and the quantities S_{AB} and S_{AB_2} refer to the amounts of minerals AB and AB_2 in their respective reaction zones. The porosity ϕ_k within the kth reaction zone is related to the mineral modal composition in the zone by the equation

$$\phi_k = 1 - \sum \phi_m. \tag{20}$$

To simplify notation, symbols a_k, b_k are introduced to represent the solute concentration within the kth reaction zone defined as follows:

$$a_k = C_A^{(k+1)}, \tag{21}$$

$$b_k = C_B^{(k+1)}, \tag{22}$$

where $C_j^{(k)}$ denotes the concentration of the jth species within the kth reaction zone as illustrated in Fig. 2 with k = 0, 1, 2, 3. In the following superscripts enclosed in round brackets (k) designate quantities internal to the kth reaction zone. The case k = 0 corresponds to the first zone in which all minerals are absent with the same fluid composition as the inlet fluid with

$$C_j^{(1)} = C_j^0. \tag{23}$$

Downstream equilibrium condition

In addition to the generalized Rankine-Hugoniot equations, the assumption of local equilibrium provides further constraints on the solute concentration within each reaction zone. To implement the condition of local equilibrium, however, is not as straightforward as it may seem. Because there is only one mineral in each reaction zone, this would provide only one additional mass action constraint for each zone, which is not enough equations to determine all the unknown quantities (see the following text). At the reaction fronts themselves, for pure advective transport the concentration is not defined because of the jump discontinuities caused by chemical reactions. This results in different values of the solute concentration depending from which side the front is approached. To resolve this ambiguity an additional assumption is required, referred to as the downstream equilibrium condition (WALSH et al., 1984; LICHTNER, 1991). According to this condition, the solute concentration downstream from each reaction front must remain in equilibrium with the mineral assemblage in the immediate upstream zone, even though it is no longer in physical contact with the minerals in that zone.

One way to understand the downstream equilibrium condition intuitively is to imagine what happens to a packet of fluid as it traverses the flow path considering both advective and diffusive transport. As the packet crosses the front $AB_2|AB$, for example, it must come to equilibrium simultaneously with both minerals AB_2 and AB located on opposite sides of the front. It is assumed that reaction kinetics are very fast so that local equilibrium is a good approximation. Furthermore, because of diffusion the fluid composition of the packet must change continuously from the upstream side of the front to the downstream side (we are considering a real fluid packet!). For very slow diffusive transport compared to advection (i.e., a large Peclet number) the concentration changes very abruptly, but nonetheless continuously, across the front. For a sufficiently small diffusion coefficient, reaction takes place only in the immediate vicinity of the front and the packet concentration is constant throughout each alteration zone. Therefore, as the packet advances further downstream it remains in equilibrium with mineral AB_2 in the upstream zone, as well as with mineral AB in the downstream zone. Thus the fluid packet is able to remember which minerals were present in the previous upstream zone. Note that the downstream equilibrium condition need not hold if the Peclet number is too small, because then internal reaction occurs, and the solute concentration is no longer constant within each zone. Actually the downstream equilibrium condition may be derived rigorously by considering transport by diffusion in addition to advection and taking the limit as the diffusion coefficient approaches zero (WALSH et al., 1984; LICHTNER, 1991).

Applying the downstream equilibrium condition to the reaction zone sequence $\mathcal{F}|AB_2|AB|A_2B$, the solute concentrations within the third and fourth zones containing minerals AB and A_2B, respectively, are invariant. Thus within zone AB the solute concentration is determined by the mass action equations

$$K_{AB_2}a_2b_2^2 = 1, \quad K_{AB}a_2b_2 = 1, \tag{24}$$

and within zone A_2B by the equations

$$K_{AB}a_3b_3 = 1, \quad K_{A_2B}a_3^2b_3 = 1. \tag{25}$$

These equations have the explicit solutions

$$a_2 = \frac{K_{AB_2}}{K_{AB}^2}, \quad b_2 = \frac{K_{AB}}{K_{AB_2}}, \tag{26}$$

and

$$a_3 = \frac{K_{AB}}{K_{A_2B}}, \quad b_3 = \frac{K_{A_2B}}{K_{AB}^2}. \tag{27}$$

The solute concentration within the second zone containing mineral AB_2 satisfies the single mass action equation

$$K_{AB_2}a_1b_1^2 = 1, \tag{28}$$

because the upstream zone contains only fluid. Note that according to Eqns. 24 and 25, the solute concentration within reaction zones AB and A_2B is in equilibrium with the mineral contained in that zone in addition to the mineral present in the immediate upstream zone.

Together the Rankine-Hugoniot equations and mass action equations provide eleven equations containing an equal number of unknowns consisting of $\{a_1, b_1, a_2, b_2, a_3, b_3, S_{AB_2}, S_{AB}, v_1, v_2, v_3\}$. For an acceptable solution to exist the mineral modal abundances and solute concentrations must all be positive, and the reaction front velocities must satisfy the inequality

$$v_1 \le v_2 \le v_3, \tag{29}$$

consistent with the assumed zone sequence. In fact, depending on the equilibrium constants chosen for minerals AB_2, AB, A_2B, and the composition of the inlet fluid, it may not be possible to find a solution to these equations which satisfies these consistency relations. In such circumstances it may be necessary to change the sequence of reaction zones considering other possibilities such as indicated in Fig. 1. Case (I) in which zone AB forms a ghost zone is of particular interest. In the pure advective limit, this situation is represented by the physically impossible relation

$$v_2 > v_3. \tag{30}$$

In this case it is necessary to alter the form of the downstream equilibrium condition to obtain a meaningful solution (SCHECHTER et al., 1987). This situation is examined further in the remainder of this section.

Mineral AB as ghost zone

To derive the condition for mineral AB to form a ghost zone, it is assumed that the terms containing the porosity in the denominators of the Rankine-Hugoniot equations can be neglected compared to the mineral volume fraction terms. The resulting equations may be solved explicitly to give the following expressions for the volume fractions of minerals AB and AB_2:

$$S_{AB} = S_{A_2B}^0 \frac{2(b_3 - b_2) - (a_3 - a_2)}{b_3 - b_2 - (a_3 - a_2)}, \tag{31}$$

and

$$S_{AB_2} = S_{AB}\frac{a_2 - a_1 - (b_2 - b_1)}{2(a_2 - a_1) - (b_2 - b_1)}, \tag{32}$$

obtained from Eqns. 18 and 19. With these relations the velocity of the third front $AB|A_2B$ may be represented by

$$v_3 = \frac{u}{S^0_{A_2B}}[a_3 - a_2 - (b_3 - b_2)], \tag{33}$$

and the velocity of the second front $AB_2|AB$ by

$$v_2 = \frac{u}{S^0_{A_2B}} \times \frac{[2(a_2 - a_0) - (b_2 - b_0)][b_3 - b_2 - (a_3 - a_2)]}{2(b_3 - b_2) - (a_3 - a_2)}. \tag{34}$$

To obtain the expression for v_2 the solute concentrations a_1 and b_1 were eliminated by using the relation

$$2a_1 - b_1 = 2a_0 - b_0, \tag{35}$$

which follows from Eqn. 17 by eliminating S_{AB_2}. The velocity v_3 and S_{AB} are independent of the composition of the inlet fluid and depend only on the invariant solute concentrations in zones AB and A_2B and the initial modal abundance of mineral A_2B. The velocity v_2 and S_{AB_2} in addition depend on the inlet fluid composition. With these relations the problem is reduced to two equations in the two unknowns a_1 and b_1, obtained by solving the conservation relation Eqn. 35 simultaneously with the mass action equation, Eqn. 28.

The threshold condition for which mineral AB first appears as a ghost zone is given by the equality of the upstream and downstream front velocities of zone AB, or

$$v_2 = v_3. \tag{36}$$

This constraint puts restrictions on the possible range of inlet fluid compositions. As follows immediately from Eqns. 33 and 34, the composition of the inlet fluid must satisfy the relation

$$2a_0 - b_0 = 3(a_2 - b_2) + 2b_3 - a_3. \tag{37}$$

The right-hand side of this equation involves only the invariant solute concentrations (a_2, b_2) and (a_3, b_3), and therefore is a function only of the equilibrium constants of minerals AB_2, AB, and A_2B. This equation defines a straight line in fluid composition space with a_0 and b_0 as axes. More generally mineral AB occurs as a ghost zone when the zone boundary velocities for pure advection satisfy the inequality

$$v_2 \geq v_3. \tag{38}$$

This implies the relation

$$2a_0 - b_0 \leq 3(a_2 - b_2) + 2b_3 - a_3, \tag{39}$$

defining a region in the inlet composition space, a_0 and b_0. As discussed in the following text, although Eqn. 38 represents a physically impossible situation, nevertheless, in the presence of diffusion this condition leads to a well-defined situation with the ghost propagating at a unique velocity.

For the other reaction zone sequences shown in Fig. 1, similar relations can be derived by equating the velocities of the respective fronts. Thus, referring to Fig. 1, the transition from the zone sequence II to III is determined by the condition

$$v_1 = v_2, \tag{40}$$

giving the requirement for disappearance of mineral AB_2, and the transition from zone III to IV by the condition

$$v_2 = v_3, \tag{41}$$

defining the threshold for disappearance of mineral AB. Only the first condition, Eqn. 36, results in a ghost zone with mineral AB trapped between minerals AB_2 and A_2B.

The regions mapped out by Eqns. 36, 40, and 41 are illustrated in Fig. 3a,b,c for three different values of the equilibrium constant $K^{-1}_{AB} = 10^{-4}$, 1.4×10^{-4}, and 1.6×10^{-4}, respectively. The reciprocal of the equilibrium constants for minerals AB_2 and A_2B are fixed at 10^{-6} and 10^{-5}, respectively. The axes correspond to the inlet concentration of solute species A and B. The regions marked I, II, III, and IV correspond to the possible reaction zone sequences shown in Fig. 1, with region I corresponding to formation of mineral AB as ghost zone. The dotted curve dividing region II in Fig. 3a and b, and regions I and II in Fig. 3c, designates the threshold condition for the absence of zone AB_2 in the initial zone sequence for pure diffusive transport. A derivation of how this curve is obtained is given in Appendix B. This curve has interesting consequences for the case of combined advection and diffusion. For initial conditions lying below the dotted curve, the zone containing mineral AB_2 is initially absent. Eventually with increasing time this zone must appear as transport becomes dominated by advection. With increasing K^{-1}_{AB}, the field for formation of AB as ghost zone (region I) increases as regions II and III decrease, and region IV increases. For $K^{-1}_{AB} > 2.15 \times 10^{-4}$, zone AB does not appear for any inlet fluid composition. The threshold value of K_{AB} for appearance of zone AB is determined by the requirement of simultaneous equilibrium with all three minerals AB, AB_2, and A_2B, leading to the relation

$$K_{AB} = (K_{AB_2}K_{A_2B})^{1/3}. \tag{42}$$

Modified downstream equilibrium condition

The common velocity v_3 for the boundaries of ghost zone AB at the threshold condition can be expressed in an alternative form which is more useful and allows generalization to multicomponent systems (see following section on multicomponent systems). From the equality of v_2 and v_3 it follows from Eqns. 18 and 19, neglecting terms containing the porosity, that

$$S_{AB} = \frac{2(a_2 - a_1)S^0_{A_2B} + (a_3 - a_2)S_{AB_2}}{a_3 - a_1} = \frac{(b_2 - b_1)S^0_{A_2B} + 2(b_3 - b_2)S_{AB_2}}{b_3 - b_1}. \tag{43}$$

This implies the relations

$$S_{AB} - S_{AB_2} = \frac{a_2 - a_1}{a_3 - a_1}(2S^0_{A_2B} - S_{AB_2}), \tag{44}$$

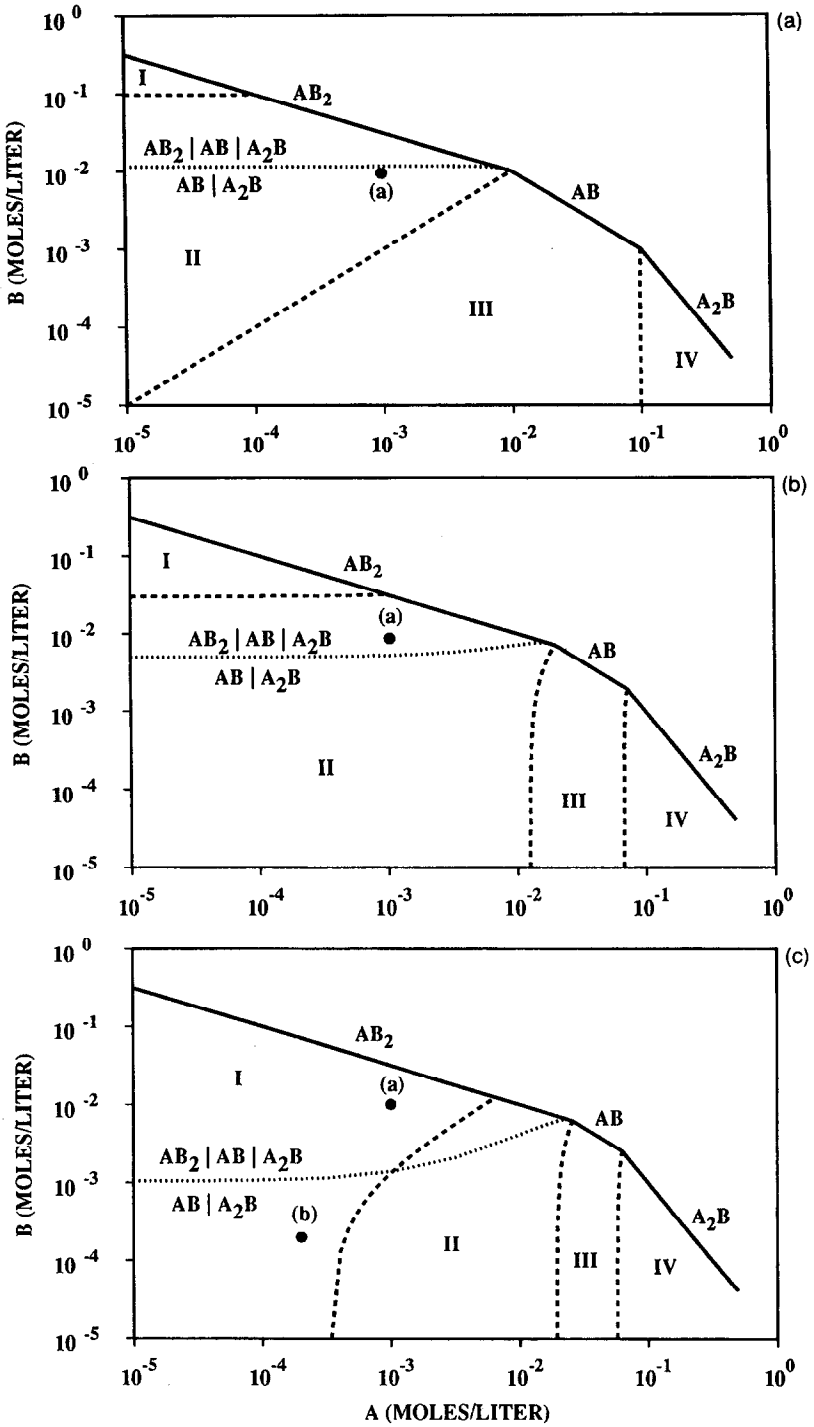

FIG. 3. The regions of occurrence of zone sequences I, II, III, and IV given in Fig. 1 as a function of the inlet fluid composition for fixed equilibrium constants of minerals AB_2 and A_2B of 10^6 and 10^5, respectively. (a) $K_{AB}^{-1} = 10^{-4}$, (b) $K_{AB}^{-1} = 1.4 \times 10^{-4}$, (c) $K_{AB}^{-1} = 1.6 \times 10^{-4}$. The dotted curve designates the threshold condition for the absence of mineral AB_2 for pure diffusive transport. The points labeled (a) and (b) correspond to inlet fluid compositions considered below.

and

$$S_{AB} - 2S_{AB_2} = \frac{b_2 - b_1}{b_3 - b_1}(S^0_{A_2B} - 2S_{AB_2}). \qquad (45)$$

Substituting these expressions into the equation for v_2 yields the following equation for the velocity of the ghost zone v_3:

$$v_3 = u\frac{a_3 - a_1}{2S^0_{A_2B} - S_{AB_2}} = u\frac{b_3 - b_1}{S^0_{A_2B} - 2S_{AB_2}}. \qquad (46)$$

This equation does not involve the solute concentration at front l_2. Combining Eqn. 46 with Eqn. 17 representing conservation of mass across the first reaction front, together with

DOWNSTEAM EQUILIBRIUM CONDITION

(I) GHOST ZONE AB

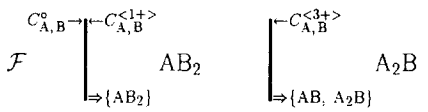

(II) NORMAL ZONE SEQUENCE

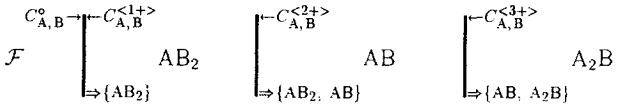

FIG. 4. Illustration of the downstream equilibrium condition for (I) sequence with AB as ghost zone, and (II) normal zone sequence. Mineral names enclosed in curly brackets are in equilibrium with the fluid downstream from the front marked by the double arrows. The single arrows designate the solute concentration on each side of the front. For the case with AB as ghost zone, mineral AB is able to buffer the fluid composition even though it is not materially present in the column.

the mass action equations Eqn. 28 and Eqn. 25, yields seven equations for the seven unknowns $\{a_1, b_1, a_3, b_3, S_{AB_2}, v_1, v_3\}$. Note that because reaction front l_2 has been eliminated, it is no longer necessary to include Eqns. 18 and 24. Accordingly, for the situation in which AB forms a ghost zone, it is possible to express the mass conservation equations in a form that does not involve mineral AB and reaction front l_2. Nevertheless, the fluid composition downstream from front l_3 is in equilibrium with minerals AB and A_2B and *not* mineral AB_2, as would be the case if the normal downstream equilibrium condition were applied directly to the zone sequence $\mathcal{F}\,|\,AB_2\,|\,A_2B$. This results in a modified downstream equilibrium condition in which mineral AB buffers the fluid composition downstream from front l_3 even though it is not materially present in the column, whence the term *ghost zone.* Mineral AB may be thought of as occupying a zone of zero thickness. In Fig. 4 the two cases corresponding to normal and modified downstream equilibrium conditions are illustrated for reaction zone sequences I and II.

Equation (46) can be further simplified. Solving for S_{AB_2} yields

$$S_{AB_2} = S^0_{A_2B}\frac{2(b_3 - b_1) - (a_3 - a_1)}{b_3 - b_1 - 2(a_3 - a_1)}. \qquad (47)$$

Eliminating S_{AB_2} from one of the equations in Eqn. 46 and making use of Eqn. 35 yields the following expression for the velocity of the ghost zone

$$v_3 = \frac{u}{3S^0_{A_2B}}[2(a_3 - a_0) - (b_3 - b_0)]. \qquad (48)$$

These relations must of course be identical to Eqns. 33 and 32 taking into account the threshold condition given by Eqn. 37. However, the equations incorporating the modified downstream equilibrium condition are more general than their derivation would suppose. They also apply when the inequality in Eqn. 38 holds. In fact this situation is the more interesting case because in a transient description incorporating advection and diffusion or dispersion, the ghost zone reaches its limiting width more rapidly (see the following text). In this case the ghost zone velocity is also a function of the inlet fluid composition in addition to the mineral equilibrium constants and the initial modal abundance of mineral A_2B. Along the threshold curve, Eqns. 33 and 48 are equivalent and in this case the ghost zone velocity is independent of the inlet fluid composition.

Three examples are considered to illustrate the theory for pure advective transport. These examples are developed further in the following text for pure diffusion and combined advection and diffusion. In the first example, $K^{-1}_{AB} = 1.4 \times 10^{-4}$ with the inlet fluid composition given by point (a) in Fig. 3b. This results in the normal zone sequence $\mathcal{F}\,|\,AB_2\,|\,AB\,|\,A_2B$. The initial volume of mineral A_2B is taken as 0.5. The molar volumes of all minerals are equal, set at 100 cm^3 $mole^{-1}$. The results are presented in Table 1. The first two rows give the solute concentration in the inlet fluid and in each of the three reaction zones. The next three rows give the volume fraction of the mineral listed in the first column, and finally the last row corresponds to the reaction front velocities at fronts l_1, l_2, and l_3 relative to the Darcy velocity u. At front l_3, mineral A_2B dissolves and is replaced by mineral AB. At front l_2, mineral AB is replaced by mineral AB_2, and at front l_1, mineral AB_2 dissolves into solution without forming any other solid phase.

In the next two examples, $K^{-1}_{AB} = 1.6 \times 10^{-4}$ with the inlet fluid composition corresponding to points (a) and (b) in Fig. 3c. In both of these cases the zone AB forms a ghost zone. The results are presented in Table 2. The pure advective description is able to give the velocities of the zone boundaries including that for the ghost zone, but cannot determine the modal abundance of mineral AB. For pure advective transport it is not possible to calculate the volume fraction of mineral AB since the width of the ghost zone is zero. In order to obtain a non-zero width and finite value for the volume fraction, it is necessary to include diffusion in the transport equations. This is carried out in the following section.

Table 1: Results of a pure advective calculation for the zone sequence $\mathcal{F}\,|\,AB_2\,|\,AB\,|\,A_2B$ for inlet concentration represented by point (a) in Fig. 3(B). The equilibrium constant of mineral AB is taken as $K^{-1}_{AB} = 1.4 \times 10^{-4}$. The zone labeled inlet corresponds to zone 1 in Fig. 2. See text for further details.

species	inlet	zone 2	zone 3	zone 4
A	0.001	0.00395	0.0196	0.0714
B	0.01	0.0159	0.00714	0.00196
φ_{AB_2}	.	0.332	.	.
φ_{AB}	.	.	0.545	.
φ_{A_2B}	.	.	.	0.5
v_k/u	.	0.00089	0.0073	0.0114

Table 2: Results of a pure advective calculation for the zone sequence $\mathcal{F} \mid AB_2 \mid < AB > \mid A_2B$ with zone AB as ghost zone for inlet concentrations represented by points (a) and (b) in Fig. 3(C). The equilibrium constant of mineral AB is taken as $K_{AB}^{-1} = 1.6 \times 10^{-4}$. The zone labeled inlet corresponds to zone 1 in Fig. 2. See text for further details.

species	inlet	zone 2	zone 3	zone 4
A	0.001	0.00395	0.0625	0.0625
B	0.01	0.0159	0.00256	0.00256
ϕ_{AB_2}	.	0.327	.	.
ϕ_{AB}	.	.	.	.
ϕ_{A_2B}	.	.	.	0.5
v_k/u	.	0.0009	0.0087	0.0087
A	0.0002	0.00637	0.0625	0.0625
B	0.0002	0.0125	0.00256	0.00256
ϕ_{AB_2}	.	0.311	.	.
ϕ_{AB}	.	.	.	.
ϕ_{A_2B}	.	.	.	0.5
v/u	.	0.00198	0.00815	0.00815

Asymptotic Width of Ghost Zone

For the two-component system and taking into account transport by diffusion, it is possible to obtain an analytic expression for the width of the ghost zone AB in the limit as time approaches infinity. For the case of combined advection and diffusion and neglecting the porosity term in the denominator, the Rankine-Hugoniot equations for the velocity of reaction front $AB|A_2B$ with position $l_3(t)$ read

$$v_3 = -\phi D \frac{[\partial C_A/\partial x]_3}{2S^0_{A_2B} - S^{\langle 3-\rangle}_{AB}} = -\phi D \frac{[\partial C_B/\partial x]_3}{S^0_{A_2B} - S^{\langle 3-\rangle}_{AB}}, \quad (49)$$

according to Eqn. 10, with the jump in solute flux given by the expression

$$[J_j]_k = -\phi D[\partial C_j/\partial x]_k. \quad (50)$$

Solving these equations for the volume fraction of mineral AB at front l_3 yields

$$S^{\langle 3-\rangle}_{AB} = S^0_{A_2B} \frac{2[\partial C_B/\partial x]_3 - [\partial C_A/\partial x]_3}{[\partial C_B/\partial x]_3 - [\partial C_A/\partial x]_3}. \quad (51)$$

Using the following relations for the partial derivatives

$$\frac{\partial C_A}{\partial x} = \frac{C_A}{C_A + C_B} \frac{\partial \chi_{AB}}{\partial x}, \quad (52)$$

and

$$\frac{\partial C_B}{\partial x} = -\frac{C_B}{C_A + C_B} \frac{\partial \chi_{AB}}{\partial x}, \quad (53)$$

derived in Appendix C (see Eqns. C9 and C10), where the quantity χ_{AB} is defined by the equation

$$\chi_{AB} = C_A - C_B, \quad (54)$$

it follows that

$$S^{\langle 3-\rangle}_{AB} = S^0_{A_2B} \frac{2C^{\langle 3\rangle}_B + C^{\langle 3\rangle}_A}{C^{\langle 3\rangle}_B + C^{\langle 3\rangle}_A}. \quad (55)$$

As a consequence, the expression for the velocity of front l_3 becomes

$$v_3 = -\frac{\phi D}{S^0_{A_2B}} \left[\frac{\partial \chi_{AB}}{\partial x}\right]_3, \quad (56)$$

as follows by substituting Eqn. 55 into Eqn. 49 and making use of Eqn. 52 or Eqn. 53.

To obtain an explicit expression for the derivative of χ_{AB}, note that within the reaction zone AB, χ_{AB} is conserved. This implies that χ_{AB} satisfies the non-reactive transport equation. In the quasi-stationary state, approximation χ_{AB} satisfies the second order ordinary differential equation

$$-\phi D \frac{d^2\chi_{AB}}{dx^2} + u \frac{d\chi_{AB}}{dx} = 0. \quad (57)$$

This equation has the solution

$$\chi_{AB} = \frac{(\chi^{\langle 3\rangle}_{AB} - \chi^{\langle 2\rangle}_{AB})e^{(x-l_2)/\lambda} - (\chi^{\langle 3\rangle}_{AB} - \chi^{\langle 2\rangle}_{AB}e^{\Delta l/\lambda})}{e^{\Delta l/\lambda} - 1}, \quad (58)$$

where Δl denotes the width of the ghost zone defined by

$$\Delta l = l_3 - l_2, \quad (59)$$

and

$$\lambda = \frac{\phi D}{u}, \quad (60)$$

denotes the characteristic diffusion length. From the expression for χ_{AB}, it follows that

$$\left(\frac{d\chi_{AB}}{dx}\right)_{x=l_3} = \frac{1}{\lambda}(\chi^{\langle 3\rangle}_{AB} - \chi^{\langle 2\rangle}_{AB}) \frac{e^{\Delta l/\lambda}}{e^{\Delta l/\lambda} - 1}. \quad (61)$$

With this result v_3 can be expressed as

$$v_3 = \frac{u}{S^0_{A_2B}}(\chi^{\langle 3\rangle}_{AB} - \chi^{\langle 2\rangle}_{AB}) \frac{e^{\Delta l/\lambda}}{e^{\Delta l/\lambda} - 1}. \quad (62)$$

Solving for Δl yields

$$\Delta l = \lambda \ln\left[\frac{f}{f-1}\right], \quad (63)$$

where the constant f is defined by

$$f = \frac{v_3 S^0_{A_2B}}{u(\chi^{\langle 3\rangle}_{AB} - \chi^{\langle 2\rangle}_{AB})}. \quad (64)$$

With increasing time the velocity of the ghost zone becomes constant, asymptotically approaching the pure advective result given by Eqn. 48. Substituting for v_3 from Eqn. 48 yields the following expression for the constant f:

$$f = \frac{2(C^{\langle 3\rangle}_A - C^0_A) - (C^{\langle 3\rangle}_B - C^0_B)}{3[C^{\langle 3\rangle}_A - C^{\langle 3\rangle}_B - (C^{\langle 2\rangle}_A - C^{\langle 2\rangle}_B)]}. \quad (65)$$

The quantity f satisfies the inequality $f > 1$, and approaches unity at the threshold for appearance of AB as a ghost zone given by Eqn. 37. Note that as $f \to 1$, the ghost zone width

$\Delta l \to \infty$. A value of infinity for the asymptotic width of the ghost zone implies that an infinite amount of time is required to achieve that width, and as a consequence the zone grows indefinitely with time.

According to Eqn. 63, the width of the ghost zone is proportional to the characteristic diffusion length λ. Thus an increase in the Darcy flow velocity u, results in a decrease in the width of the ghost zone. The function f depends on the inlet fluid composition and mineral equilibrium constants. The asymptotic width of the ghost zone is independent of the initial volume fraction of mineral A_2B, as well as the mineral molar volumes. In the case of dispersive transport, the dispersion coefficient is proportional to the fluid velocity. In this case λ is equal to the characteristic dispersion length of the system and is independent of the fluid flow velocity. Under such circumstances the width of the ghost zone is constant across a region of changing permeability provided the dispersion length is constant. These properties may be useful for identifying such zones in the field. Conversely, measurement of the width of a ghost zone may serve to determine the local Darcy velocity or dispersivity.

Within the ghost zone the asymptotic form of the solute concentration profile is given by the equations

$$C_A = (\chi_{AB} + [\chi_{AB}^2 + 4K_{AB}^{-1}]^{1/2})/2, \tag{66}$$

and

$$C_B = (-\chi_{AB} + [\chi_{AB}^2 + 4K_{AB}^{-1}]^{1/2})/2, \tag{67}$$

as derived in Appendix C. The asymptotic profile of the volume fraction of ghost zone mineral AB can be determined by integrating the mineral mass transfer equation

$$\frac{\partial \phi_m^{(k)}}{\partial t} = \bar{V}_m I_m^{(k)}, \tag{68}$$

where the internal reaction rate $I_m^{(k)}$ is obtained from the solute transport equations within the kth reaction zone. Transforming this equation to a coordinate system (x', t') at rest with respect to the ghost zone according to

$$x' = x - v_3 t, \tag{69}$$

and

$$t' = t, \tag{70}$$

yields

$$\frac{\partial S_{AB}}{\partial t} = -v_3 \frac{\partial S_{AB}}{\partial x'} + \frac{\partial S_{AB}}{\partial t'}. \tag{71}$$

The term $\partial S_{AB}/\partial t'$ vanishes at steady-state resulting in the equation

$$\frac{dS_{AB}}{dx'} = -\frac{1}{v_3} \mathcal{I}_{AB}(x'), \tag{72}$$

where the reaction rate $\mathcal{I}_{AB}$ is given by Eqn. C20. Integrating this equation gives

$$S_{AB}(x') = S_{AB}(\Delta l) + \frac{1}{v_3} \int_{x'}^{\Delta l} \mathcal{I}_{AB}(x'')dx'', \tag{73}$$

where

$$S_{AB}(\Delta l) = S_{AB}^{\langle 3- \rangle}, \tag{74}$$

from which the spatial dependence of the volume fraction of mineral AB is determined.

Numerical Examples

To investigate the time evolution of a ghost zone and its approach to a constant, asymptotic width, it is necessary to solve the transport equations numerically taking into account transport by advection and diffusion. The correct solution to the transport equations for pure diffusion was given only recently by NOVAK et al. (1989) and BALASHOV and LEBEDEVA (1991). LICHTNER (1991) presented a numerical solution for combined advection and diffusion based on the quasi-stationary state approximation. For the calculations presented below in all cases $K_{AB_2}^{-1} = 10^{-6}$ and $K_{A_2B}^{-1} = 10^{-5}$. In addition, a Darcy velocity of $u = 10^{-6}$ cm sec^{-1}, a diffusion coefficient of $D = 10^{-5}$ cm^2 sec^{-1}, and a porosity of $\phi = 0.1$ is assumed in the calculations. The initial volume fraction of mineral A_2B is taken as $\phi_{A_2B} = 0.5$, and the molar volumes of all minerals equal to 100 cm^3 mole^{-1}. The initial solution composition is assumed to be invariant in equilibrium with minerals AB and A_2B. This assumption eliminates internal reaction within zone A_2B.

First consider the case where the normal zone sequence $\mathcal{I}|AB_2|AB|A_2B$ occurs. This is shown in Figs. 5–7 for $K_{AB}^{-1} = 1.4 \times 10^{-4}$ with the inlet fluid composition given by the point labeled (a) in Fig. 3(B) corresponding to $C_A^0 = 10^{-3}$ and $C_B^0 = 10^{-2}$ mol L^{-1}. The solution for pure diffusion is used to start the combined advection and diffusion calculation. The mineral volume fractions for pure diffusion corresponding to the early time behavior of the system are shown in Fig. 5 as functions of the similarity variable η (see Appendix B). Internal reaction results in the characteristic shapes of the profiles for zones AB_2 and AB. Internal reaction does not take place in zone A_2B because of the choice of initial conditions. The positions of the reaction zone boundaries $l_k(t)$ are plotted as a function of time in Fig. 6. As can be seen

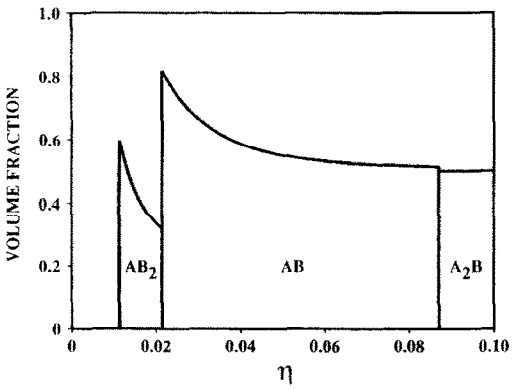

FIG. 5. The modal abundances of minerals AB_2, AB, and A_2B plotted as a function of the similarity variable η for the case of pure diffusive transport. The parameters used in the calculation are $D = 10^{-5}$ cm^2 sec^{-1}, $\phi = 0.1$, $S_{A_2B}^0 = 0.5$, $K_{AB}^{-1} = 1.4 \times 10^{-4}$, $K_{AB_2}^{-1} = 10^{-6}$, and $K_{A_2B}^{-1} = 10^{-5}$.

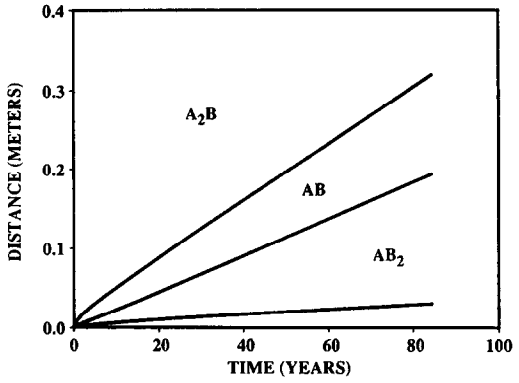

FIG. 6. The reaction zone boundaries of minerals AB_2, AB, and A_2B plotted as a function of the time for combined advection and diffusion with a Darcy velocity of $u = 10^{-6}$ cm sec^{-1} and otherwise the same parameters as used in Fig. 5. The composition of the inlet fluid corresponds to point (a) in Fig. 3b.

from the figure, the width of zone AB, as well as the other zones, increases with increasing time. The velocities of the zone boundaries given by the slopes of the curves $l_k(t)$ asymptotically approach constant values resulting in a steady-state. The values obtained from the figure after an elapsed time of 80 years are approximately 9.08×10^{-4}, 7.36×10^{-3}, and 1.14×10^{-2} relative to the Darcy velocity u. These values are in good agreement with the values obtained from the pure advective transport equations given in Table 1.

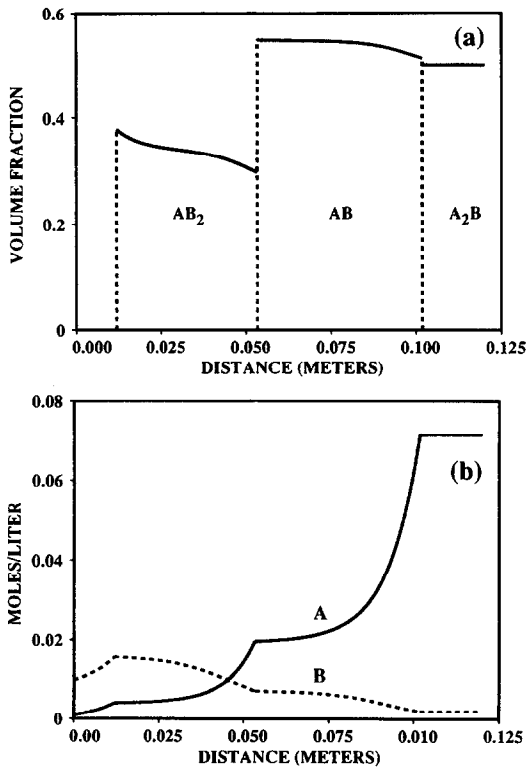

FIG. 7. (a, b) Mineral modal abundances and concentrations of solute species A and B plotted as a function of distance for the same conditions as in Fig. 6 and for an elapsed time of approximately 24 years.

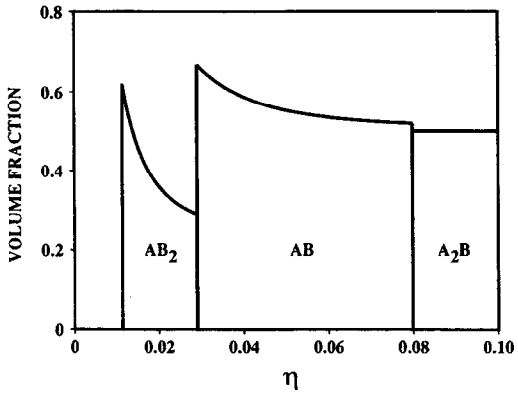

FIG. 8. The modal abundances of minerals AB_2, AB, and A_2B plotted as a function of the similarity variable η for the case of pure diffusive transport. The inlet conditions correspond to point (a) in Fig. 3c. The equilibrium constant for mineral AB has the value $K_{AB}^{-1} = 1.6 \times 10^{-4}$ with otherwise the same parameters as used in the previous example.

The mineral modal abundances are plotted in Fig. 7(a) as a function of distance after an elapsed time of approximately 24 years. The volume fractions within zones AB_2 and AB approach a constant value given by the pure advective limit. The average values of the volume fractions are in good agreement with the values in Table 1. The concentrations of solute species A and B in zones AB_2 and AB are shown in Fig. 7b as a function of distance for the same time. The concentration becomes constant towards the upstream side of each zone, and rapidly approaches the invariant concentration on the downstream side. In the limit as the diffusion coefficient vanishes, the solute concentration profiles approach chemical shock fronts with jump discontinuities at the downstream side.

Figures 8–11 depict the formation of ghost zone AB for $K_{AB}^{-1} = 1.6 \times 10^{-4}$ for the same inlet fluid composition given in the previous example corresponding to the point labeled (a) in Fig. 3c. For these conditions the initial zone sequence is $\mathcal{F} \mid AB_2 \mid AB \mid A_2B$ according to Fig. 3c. The corresponding

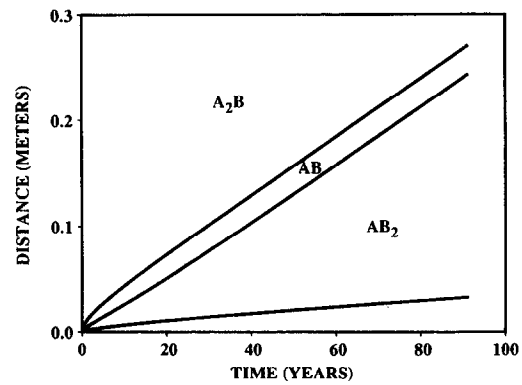

FIG. 9. The reaction zone boundaries of minerals AB_2, AB, and A_2B plotted as a function of the time for combined advection and diffusion with a Darcy velocity of $u = 10^{-6}$ cm sec^{-1} and otherwise the same parameters as used in Fig. 8. In this case, zone AB forms a ghost zone which propagates with constant width after a sufficiently long time interval has elapsed.

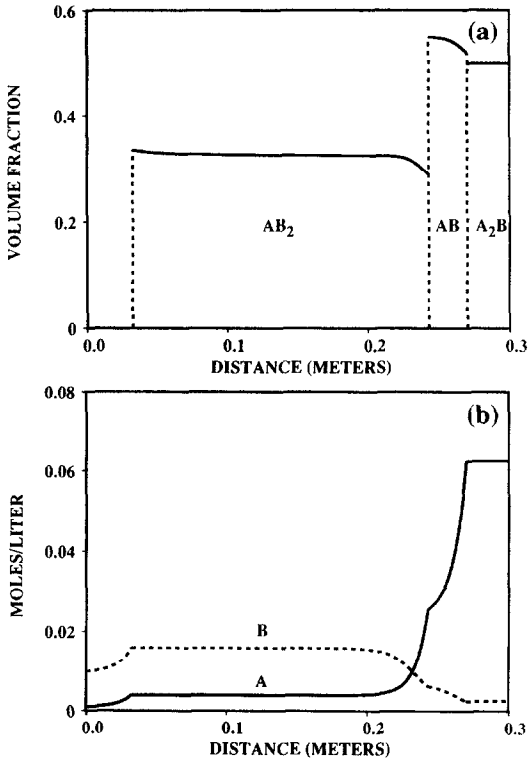

FIG. 10. (a, b) Mineral modal abundances and concentrations of solute species A and B plotted as a function of distance for the same conditions as in Fig. 9 for an elapsed time of approximately 91 years.

diffusion profile of the mineral modal abundances is shown in Fig. 8 plotted as a function of the similarity variable η. The positions of the zone boundaries as a function of time are shown in Fig. 9. As is apparent from the figure the width of zone AB becomes constant after a relatively short time interval has elapsed. The velocities of the reaction fronts obtained from the numerical calculation after a sufficiently long period of time has elapsed are in good agreement with the pure advective limit given in Table 2 based on the modified downstream equilibrium condition. According to the figure,

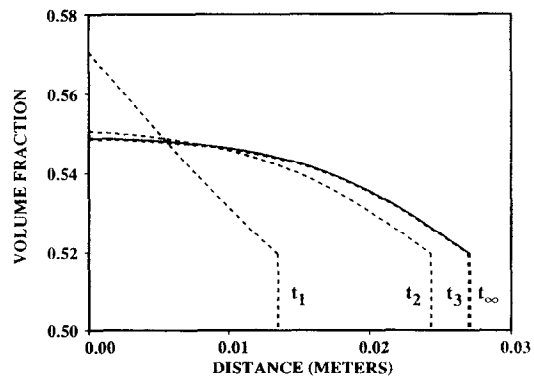

FIG. 11. The volume fraction of ghost zone AB plotted as a function of distance for various times (t_1 = 5.44, t_2 = 27.94, t_3 = 91.36, and $t_\infty = \infty$ years) indicated in the figure showing its approach to a constant width and shape with increasing time. The profile for $t \to \infty$ is calculated from Eqn. 73. The same conditions as in the previous figure are used.

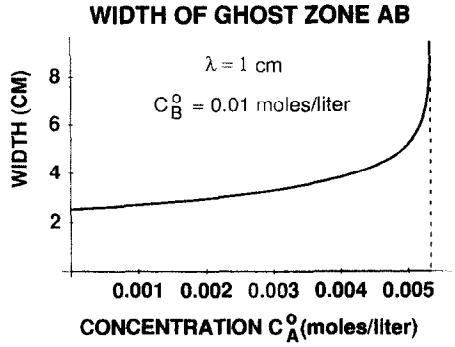

FIG. 12. The asymptotic width of ghost zone AB plotted as a function of the inlet concentration of species A for a fixed value of $C_B^0 = 10^{-2}$ mol L^{-1} for $K_{AB}^{-1} = 1.6 \times 10^{-4}$.

the relative reaction front velocities v_k/u after an elapsed time of approximately 90 years are approximately 9.15 $\times 10^{-4}$ and 8.70 $\times 10^{-3}$. The mineral modal abundances and solute concentrations are shown in Fig. 10a and b, respectively. Within the ghost zone AB the concentration profile remains controlled by diffusive transport. The time evolution of ghost zone AB is shown in Fig. 11 where the volume fraction of AB is plotted as a function of distance for the indicated times for a coordinate system fixed at the upstream boundary of the ghost zone. The asymptotic width and volume fraction profile of the ghost zone calculated from Eqns. 63 and 73 are in good agreement with the numerical calculation.

To investigate the behavior of the width of the ghost zone on the inlet fluid composition, in Fig. 12 the asymptotic width is plotted as a function of the inlet concentration of species A for fixed concentration of species B. The width approaches infinity as C_A^0 approaches the threshold for the onset of the ghost zone of 0.005335 mol L^{-1}, indicated by the vertical dashed line. Thus precisely at the threshold for formation of a ghost zone, the ghost actually grows continuously with time and its width never reaches a constant value.

Figures 13–17 depict the formation of ghost zone AB for the initial condition given by point (b) in Fig. 3c corresponding to $C_A^0 = C_B^0 = 2 \times 10^{-4}$ mol L^{-1}. In this case, the initial

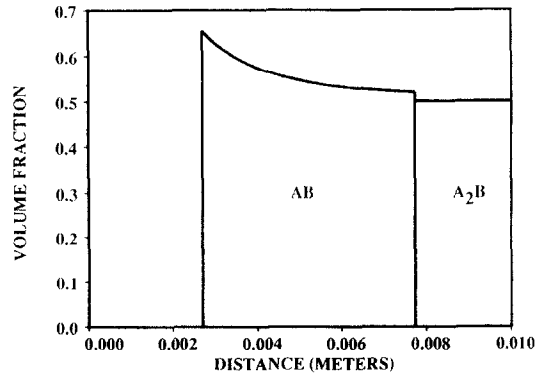

FIG. 13. The modal abundances of minerals AB and A_2B plotted as a function of the similarity variable η for the case of pure diffusive transport. The inlet conditions correspond to point (b) in Fig. 3c with otherwise the same parameters as used in the previous example. The mineral AB_2 does not appear for transport by pure diffusion.

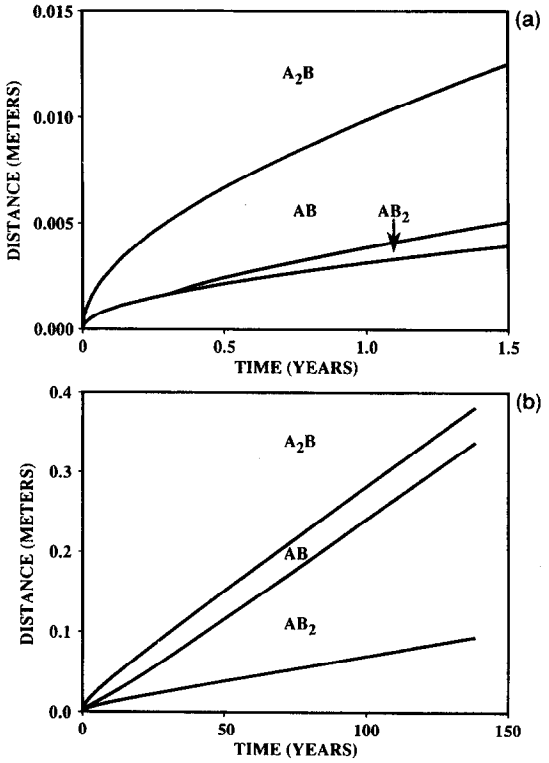

FIG. 14. The reaction zone boundaries of minerals AB_2, AB, and A_2B plotted as a function of the time for combined advection and diffusion with a Darcy velocity of $u = 10^{-6}$ cm sec^{-1} and otherwise the same parameters as used in Fig. 13. (a) The reaction zone boundaries shown for times up to 1.5 years. Mineral AB_2 first appears after an elapsed time of approximately 0.3 years. (b) The reaction zone boundaries shown for times up to 140 years. Zone AB forms a ghost zone.

zone sequence is $\mathcal{F}|AB|A_2B$ according to Fig. 3. The pure diffusion profiles for the mineral modal abundances are shown in Fig. 13. The positions of the zone boundaries as a function of time are shown in Fig. 14a and b. Zone AB_2 appears after approximately 0.3 years have elapsed. With increasing time, zone AB propagates at constant width as can be seen in Fig. 14b. The reaction front velocities are shown

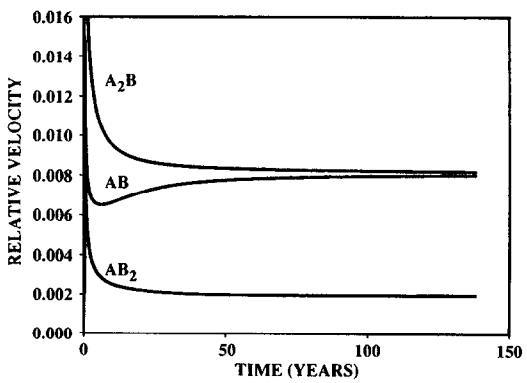

FIG. 15. Relative reaction front velocities plotted as a function of time for the same conditions as in Fig. 14. With increasing time the velocities of boundaries of zone AB become equal characteristic of the property of a ghost zone.

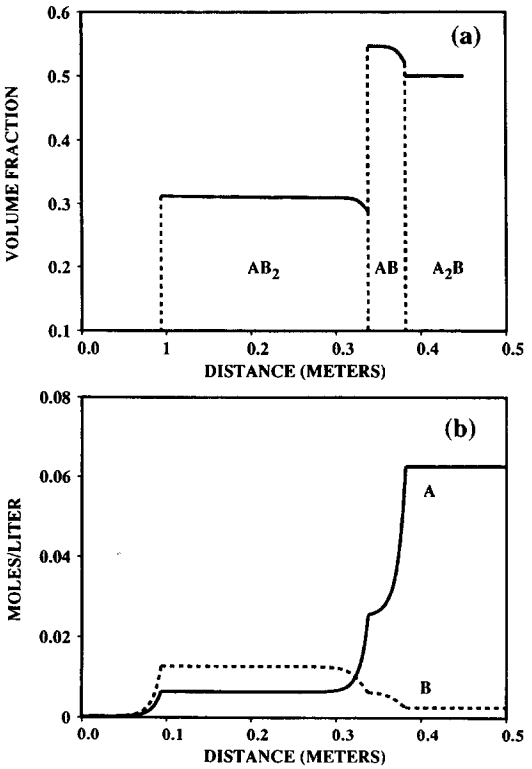

FIG. 16. (a, b) Mineral modal abundances and concentrations of solute species A and B plotted as a function of distance for the same conditions as in Fig. 14 after an elapsed time of approximately 140 years.

in Fig. 15. The values of the relative velocities v_k/u after an elapsed time of 200 years of 1.98×10^{-3}, 8.08×10^{-3}, and 8.22×10^{-3} are in excellent agreement with the asymptotic values for pure advective transport given in Table 2. The modal abundance and solute concentrations are shown in Fig. 16a and b. The time evolution of the ghost zone AB is shown in Fig. 17. In this case a longer time is required for a steady state to be established compared to the previous example.

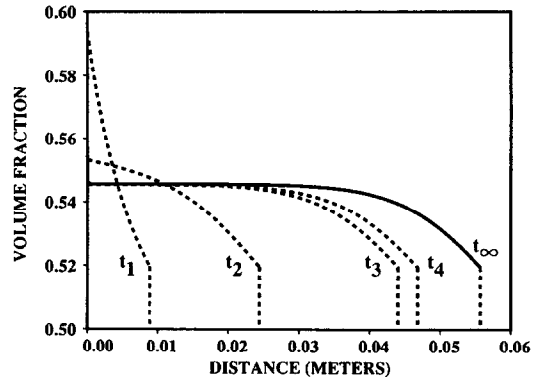

FIG. 17. The volume fraction of ghost zone AB plotted as a function of distance for various times ($t_1 = 2.13$, $t_2 = 17.04$, $t_3 = 138.49$, $t_4 = 199.47$, and $t_\infty = \infty$ years) indicated in the figure showing its approach to a constant width and shape with increasing time. The profile for $t = \infty$ is calculated from Eqn. 73.

MULTICOMPONENT SYSTEM

Modified Downstream Equilibrium Condition

The same considerations leading to the modified downstream equilibrium condition for a two-component system also apply to a multicomponent system. This section considers the general case of a multicomponent system in which both homogeneous and heterogeneous reactions may take place described by the reactions

$$\sum_j \nu_{ji}^{aq} \mathcal{A}_j \rightleftharpoons \mathcal{A}_i, \tag{75}$$

to form the aqueous complex $\mathcal{A}_i$, and

$$\sum_j \nu_{jm} \mathcal{A}_j \rightleftharpoons \mathcal{M}_m, \tag{76}$$

for mineral $\mathcal{M}_m$. The species $\mathcal{A}_j$ occurring on the left-hand side of these reactions represent an independent set of solute species referred to as primary species. The quantities ν_{jm} and ν_{ji}^{aq} denote the stoichiometric reaction coefficients for minerals and aqueous complexes, respectively. The Rankine-Hugoniot equations can be expressed in the form (LICHTNER, 1991)

$$v_k = \frac{[\Omega_j]_k}{[\phi \Psi_j]_k + \sum_m \nu_{jm} [S_m]_k}, \tag{77}$$

analogous to Eqn. 10 for the two-component system, where Ψ_j denotes the generalized concentration defined within the kth reaction zone by

$$\Psi_j^{(k)} = C_j^{(k)} + \sum_i \nu_{ji}^{aq} C_i^{(k)}, \tag{78}$$

where $C_j^{(k)}$ and $C_i^{(k)}$ denote the concentration of the jth primary species and ith aqueous complex, respectively, and $\Omega_j^{(k)}$ denotes the generalized flux defined by

$$\Omega_j^{(k)} = J_j^{(k)} + \sum_i \nu_{ji}^{aq} J_i^{(k)}, \tag{79}$$

where $J_j^{(k)}$ and $J_i^{(k)}$ denote the flux of the jth primary species and ith complex, respectively, defined in Eqn. 5. For pure advective transport

$$\Omega_j^{(k)} = u \Psi_j^{(k)}. \tag{80}$$

To these equations must be added the downstream equilibrium condition stating that the fluid composition within each reaction zone is in equilibrium with the minerals in the zone, in addition to being in equilibrium with the mineral assemblage in the neighboring upstream zone. This results in the mass action equations

$$K_m \prod_j (\gamma_j^{(k)} C_j^{(k)})^{\nu_{jm}} = 1, \tag{81}$$

where the subscript m runs over all minerals present in both the kth and $k-1$st reaction zones.

To derive the form of the Rankine-Hugoniot equations when a zone of zero width is present, consider the situation in which the kth reaction zone forms a ghost zone. At the threshold for ghost zone formation, the velocities of the kth and $k-1$st reaction fronts which border the kth zone must be equal:

$$v_k = v_{k-1}. \tag{82}$$

This implies the relation

$$\frac{[\Psi_j]_k}{\sum \nu_{jm} [S_m]_k} = \frac{[\Psi_j]_{k-1}}{\sum \nu_{jm} [S_m]_{k-1}}, \tag{83}$$

as follows from Eqn. (77) neglecting terms containing the porosity in the denominator. Solving this equation for $\sum_m \nu_{jm} S_m^{(k)}$ yields the result

$$\sum_m \nu_{jm} S_m^{(k)} = \frac{[\Psi_j]_k \sum_m \nu_{jm} S_m^{(k-1)} + [\Psi_j]_{k-1} \sum_m \nu_{jm} S_m^{(k+1)}}{[\Psi_j]_k + [\Psi_j]_{k-1}}. \tag{84}$$

Noting that from the definition of the square brackets $[\cdots]$ it follows that

$$[\Psi_j]_k + [\Psi_j]_{k+1} = \Psi_j^{(k+1)} - \Psi_j^{(k-1)}, \tag{85}$$

the equation for v_k becomes

$$v_k = u \frac{\Psi_j^{(k+1)} - \Psi_j^{(k-1)}}{\sum \nu_{jm} (S_m^{(k+1)} - S_m^{(k-1)})}. \tag{86}$$

Therefore, the Rankine-Hugoniot equations can be expressed in a form in which the kth zone is missing from the expression for v_k. Applying the downstream equilibrium condition in the usual way, taking into account the kth zone of zero width, implies that the fluid in the $k+1$st zone must be in equilibrium with the minerals in the kth zone, this in spite of the fact that its width is zero. Thus whenever a ghost zone occurs in the reaction zone sequence, mass balance equations are calculated as if this zone did not appear, while mineral mass action equations must take into account the presence of minerals in the ghost zone. This result may be further generalized to the occurrence of n consecutive ghost zones beginning with the kth zone. In this case mass balance constraints apply between the $k-1$st and $k+n$th zones, while mass action constraints apply to minerals in the $k+n-1$st zone and the $k+n$th zone. The intervening $n-1$ ghost zones, labeled $k, k+1, \ldots, k+n-2$, do not affect the mass conservation equations or the mass action equations, and therefore do not influence the solution to the pure advective mass transport equations. Note, however, that there may exist special situations where the above analysis does not apply (LICHTNER and WABER, 1992).

Existence of Solutions and Kinetics

Aside from their possible geochemical significance, the presence of ghost zones has important implications on the existence and properties of solutions to the mass transport equations in the limiting case of pure advection, for conditions of local equilibrium and surface controlled reactions. The pure advective transport equations represent an attractive simplification compared to a description including diffusion or dispersion. This is because a pure advective description and that for combined advection-diffusion/dispersion yield similar solutions for sufficiently large time spans (LICHTNER, 1992b). However, the pure advective case is computationally much more efficient. For conditions of local equilibrium in

an isothermal system, the pure advective transport equations result in a system of non-linear, algebraic equations that need only be solved once for all time. For surface controlled mineral reactions within the quasi-stationary state approximation, the pure advective transport equations require solving a set of first order, ordinary differential equations (LICHTNER, 1988). While either of these equations is far easier to solve than the corresponding second order differential equations that result if diffusive transport is included, nevertheless, the existence of ghost zones greatly limits the usefulness of the pure advective limit. For conditions of local equilibrium and pure advective transport, a ghost zone has zero width; and it is not possible to determine the modal abundance of minerals in the ghost zone. Although a solution to the transport equations for pure advection always exists in a kinetic description of mineral reaction rates, the width of the ghost zone is an artifact of the choice of kinetic rate constants and must tend to zero as the rate constants approach infinity. By contrast, if diffusion is included in the kinetic description the width of the ghost zone tends to a non-zero limiting value in agreement with the local equilibrium formulation. In many ways, a kinetic approach is computationally superior to local equilibrium. First, because the difficulties associated with determining the sequence of reaction zones, which in a local equilibrium description require trial and error methods, disappear. And second, a kinetic description contains local equilibrium as a special case as the kinetic rate constants tend towards infinity.

For transport by diffusion and advection, as first pointed out by KORZHINSKII (1970), a solution to the transport equations always exists. It is to be expected that diffusion should be an important factor in describing the properties of ghost zones because of their vanishing width in the pure advective limit. For structures in solute and mineral concentration profiles with length scales on the order of, or less than, the characteristic diffusion length of the system, transport by diffusion must play an important role. These considerations also apply to the sharp reaction fronts obtained for pure advective transport in the form of chemical shock waves. Nevertheless, certain properties of ghost zones can be investigated in the limit as the diffusion coefficient vanishes resulting in pure advective transport.

The Possible Existence of Ghost Zones

A basic characteristic of mineral reaction fronts is that they move extremely slowly compared to the fluid flow velocity. This presents a difficult problem to determine from field observations whether a zone is advancing with constant width, or is increasing or perhaps decreasing in width. The fundamental property of ghost zones that their width is inversely proportional to the fluid flow rate and directly proportional to the diffusion or dispersion coefficient suggests a possible means for observing such zones in natural systems. For a situation in which the permeability, and hence fluid flow rate, varies spatially over a region in which the host rock has a relatively uniform composition (so that chemical reactions could be presumed the same at neighboring points), the appearance of a ghost zone would manifest itself by exhibiting a behavior that was distinct from normal zones. In regions of higher permeability the width of normal zones would be larger compared to regions of lower permeability. By contrast the width of a ghost zone would either be more narrow in regions of higher permeability compared to regions of lower permeability, or remain the same independent of the fluid flow velocity. This latter situation would occur in the case of dispersive transport since the dispersion coefficient is proportional to the fluid velocity.

Ghost zones have been shown to occur in several numerical calculations involving multicomponent geochemical systems applied to weathering and supergene enrichment of a porphyry copper deposit (LICHTNER and WABER, 1992; LICHTNER and BIINO, 1992). Another possible occurrence of ghost zones may be in the formation of bauxite deposits. It has been observed that in bauxite deposits the maximum width of the kaolinite zone may vary over several orders of magnitude for different deposits ranging from millimeters to tens of meters or more for comparable sized zones containing bauxite ore (GORDON et al., 1985). A possible explanation of this observation is that the kaolinite zone forms a ghost zone for those deposits where it is more narrow. As noted by LICHTNER (1991), with decreasing P_{CO_2}, or equivalently increasing pH by charge balance, the kaolinite zone formed from the weathering of K-feldspar becomes a ghost zone. This is demonstrated in Fig. 18 where the ratio of the upstream to downstream reaction front velocities of the kaolinite zone is plotted as a function of the P_{CO_2} of the inlet fluid for two different log K values for kaolinite corresponding to 7.0 and 7.4. A ratio of less than one corresponds to a consistent solution, whereas a ratio greater than one implies that kaolinite forms a ghost zone. The threshold value unity designates the onset of ghost zone behavior. In this case the actual width and modal abundance of the kaolinite zone can only be determined by including transport by diffusion and dispersion in the calculation. One possible mechanism to explain the variation in the P_{CO_2} could be different soil compositions ranging from sandy or gravelly soil to silty or clayey soils. However, a much more detailed investigation of individual sites would be necessary to confirm this hypothesis. There are also other plausible explanations. For example, the drastic

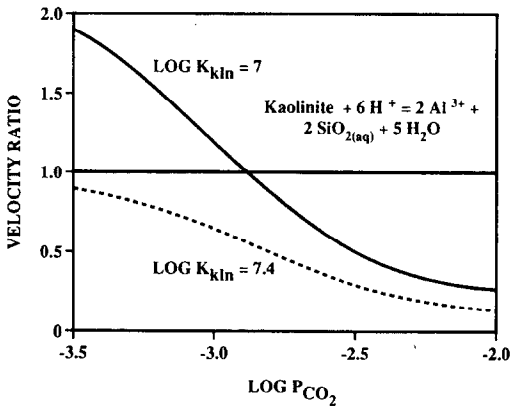

FIG. 18. The ratio of upstream to downstream reaction front velocities of the kaolinite zone in the weathering of K-feldspar plotted as a function of the P_{CO_2} of the inlet fluid for two different Log K values. A ratio greater than one corresponds to the kaolinite forming a ghost zone.

change in permeability across the saprolite-unaltered rock interface causing deflection of downward percolating water could be responsible for these observations.

CONCLUSION

The existence of reaction zones which propagate with constant width, referred to as ghost zones, has been demonstrated for a simple two-component system. An analytical expression for the asymptotic width of the ghost was derived by considering transport by advection and diffusion. For conditions of local chemical equilibrium of mineral reactions, there may exist no physically acceptable solutions to mass transport equations representing pure advection. It was demonstrated that by modifying the downstream equilibrium condition in some cases a consistent solution could be found which agreed with numerical calculations for reaction front velocities of the ghost zone. However, it is not possible to calculate the width or modal composition of the ghost zone without taking into account diffusive transport. The pure advective kinetic transport equations yield the correct reaction front velocities in agreement with the local equilibrium limit, but the predicted width of a ghost zone is an artifact of the kinetic rate constants used in the calculation. Nevertheless, a kinetic description provides much greater flexibility than the assumption of local equilibrium and is to be preferred.

Editorial handling: F. A. Frey

REFERENCES

BALASHOV V. N. (1985) On a mathematical description of metasomatic zoning with multicomponent minerals. *Dokl. Akad. Nauk SSSR* **280,** 746–750 (in Russian).

BALASHOV V. N. and LEBEDEVA M. I. (1991) Macrokinetic model of the origin and development of a monomineralic bimetasomatic zone. *Progress in Metamorphic and Magmatic Petrology; A memorial volume in honor of D. S. Korzhinskii* (ed. L. L. PERCHUK), pp. 167–195. Cambridge University Press.

BALASHOV V. N. and LICHTNER P. C. (1991) Disappearing zones in infiltration metasomatic zoning. *Dokl. Akad. Nauk SSSR* **321,** 1242–1246 (in Russian).

GORDON M. J., TRACY J. I., and ELLIS M. W. (1985) Geology of the Arkansas bauxite region. *Geol. Survey Prof. Paper* **299,** 268 pp.

KORZHINSKII D. S. (1970) *Theory of Metasomatic Zoning* (trans. J. AGRELL). Clarendon Press.

LASAGA A. C. (1984) Chemical kinetics of water-rock interaction. *J. Geophys. Res.* **89,** 4009–4025.

LICHTNER P. C. (1985) Continuum model for simultaneous chemical reactions and mass transport in hydrothermal systems. *Geochim. Cosmochim. Acta* **49,** 779–800.

LICHTNER P. C. (1988) The quasi-stationary state approximation to coupled mass transport and fluid-rock interaction in a porous medium. *Geochim. Cosmochim. Acta* **52,** 143–165.

LICHTNER P. C. (1991) The quasi-stationary state approximation to fluid-rock reaction: Local equilibrium revisited. *Advances in Phys. Geochem.* **8,** 454–562.

LICHTNER P. C. (1992a) Scaling properties of kinetic mass transport equations and the local equilibrium limit. *Amer. J. Sci.* (submitted).

LICHTNER P. C. (1992b) Time-space continuum description of fluid-rock interaction in permeable media. *Water Resources Res.* (in press)

LICHTNER P. C. and BIINO G. G. (1992) A first principles approach to supergene enrichment of a porphyry copper protore. I. Cu-Fe-S-H_2O subsystem. *Geochim. Cosmochim. Acta* **56,** 3987–4013.

LICHTNER P. C. and WABER N. (1992) Redox front geochemistry and weathering: Theory with application to the Osamu Utsumi uranium mine, Poços de Caldas, Brazil. *J. Geochem. Exp.* (in press).

MERINO E., MOORE C., ORTOLEVA P., and RIPLEY E. (1986) Mineral zoning in sediment-hosted copper-iron sulfide deposits—A quantitative kinetic approach. In *Geology and Metallogeny of Copper Deposits* (ed. G. H. FRIEDRICH et al.); Special Publication No. 4 of the Soc. Geo. App. Min. Dep., Proceedings of the Copper Symposium 27th International Congress Moscow, 1984, pp. 559–571. Springer-Verlag.

NOVAK C. F., SCHECHTER R. S., and LAKE L. W. (1989) Diffusion and solid dissolution/precipitation in permeable media. *AIChE J.* **35,** 1057–1072.

SCHECHTER R. S., BRYANT S. L., and LAKE L. W. (1987) Isotherm-free chromatography: Propagation of precipitation/dissolution waves. *Chem. Eng. Comm.* **58,** 353–376.

STEEFEL C. I. and VAN CAPPELLEN P. (1990) A new kinetic approach to modeling water-rock interaction. The role of nucleation, precursors, and Ostwald ripening. *Geochim. Cosmochim. Acta* **54,** 2657–2677.

WALSH M. P., BRYANT S. L., SCHECHTER R. S., and LAKE L. W. (1984) Precipitation and dissolution of solids attending flow through porous media. *Amer. Inst. Chem. Eng. J.* **30,** 317–327.

APPENDIX A

Internal Reaction and the Quasi-Stationary State Approximation

In this appendix equations are derived to determine the mineral modal abundance within an alteration zone for conditions of local equilibrium taking into account advective and diffusive transport. Consider the monomineralic sequence of reaction zones $\mathcal{F}|AB_2|AB|A_2B$ as illustrated in Fig. 2. It is essential to take into account internal reaction whenever diffusion is included in the description. Otherwise the correct asymptotic behavior as the solution approaches the pure advective limit of the transport equations cannot be obtained (LICHTNER, 1991). The Rankine-Hugoniot equations may be solved explicitly for the mineral modal compositions $S_{AB_2}^{\langle 2-\rangle}$ and $S_{AB}^{\langle 3-\rangle}$ at fronts l_2 and l_3, respectively, to yield

$$S_{AB_2}^{\langle 2-\rangle} = S_{AB}^{\langle 2+\rangle} \frac{[J_A]_2 - [J_B]_2}{2[J_A]_2 - [J_B]_2}, \tag{A1}$$

and

$$S_{AB}^{\langle 3-\rangle} = S_{A_2B}^{\langle 3+\rangle} \frac{[J_A]_3 - 2[J_B]_3}{[J_A]_3 - [J_B]_3}. \tag{A2}$$

For the special choice of invariant initial conditions, the concentration of mineral AB at boundary l_3 reduces to a constant given by

$$S_{AB}^{\langle 3-\rangle} = S_{A_2B}^{0} \frac{C_A^{\langle 3\rangle} + 2C_B^{\langle 3\rangle}}{C_A^{\langle 3\rangle} + C_B^{\langle 3\rangle}}. \tag{A3}$$

To determine $S_{AB_2}^{\langle 2-\rangle}$ from Eqn. A1 it is first necessary to know $S_{AB}^{\langle 2+\rangle}$, the value of the volume fraction of mineral AB at its upstream boundary l_2. This can be computed as follows. Alteration of the mth mineral within the kth reaction zone is described by Eqn. 68. According to Eqn. 4 an expression for the internal reaction rate can be derived given by

$$I_m^{(k)} = \frac{\partial S_m^{(k)}}{\partial t} = \frac{1}{\nu_{jm}} \left\{ -\frac{\partial \phi C_j^{(k)}}{\partial t} + \frac{\partial}{\partial x}\left(\phi D \frac{\partial C_j^{(k)}}{\partial x}\right) - u\frac{\partial C_j^{(k)}}{\partial x} \right\}. \tag{A4}$$

Integrating Eqn. 68 gives the modal abundance of the mth mineral at a fixed distance from the inlet as a function of time according to the expression

$$S_m^{(k)}(x, t) = S_m^{(k)}(x, \tau_k(x)) + \int_{\tau_k(x)}^{t} I_m^{(k)}(x, t')dt', \tag{A5}$$

where the lower limit of integration $\tau_k(x)$ denotes the instant at which

the downstream boundary of the kth reaction zone arrives at the observation point x, or in symbols

$$l_k(\tau_k(x)) = x. \tag{A6}$$

To obtain the value of $S_m^{(k)}$ at its upstream boundary l_{k-1} at time t, x in Eqn. A5 is replaced by $l_{k-1}(t)$ and the upper limit of integration t by the time required for the front l_{k-1} to arrive at the position $l_{k-1}(t)$. This gives the expression

$$S_m^{(k)}(l_{k-1}(t), t) = S_m^{(k)}(l_{k-1}(t), \tau_k(l_{k-1})) + \int_{\tau_k(l_{k-1}(t))}^{\tau_{k-1}(l_{k-1}(t))} I_m^{(k)}(l_{k-1}(t), t')dt'. \tag{A7}$$

Note that $\tau_{k-1}(l_{k-1}(t)) \geq \tau_k(l_{k-1}(t))$, since at the time the $k-1$st front arrives at the position l_{k-1}, the kth front has already passed this position and has arrived at l_k.

As an example of the evaluation of $\tau_k(x)$ consider the situation of pure diffusive transport for which the position of the front is given by

$$l_k(t) = 2\eta_k\sqrt{Dt}, \tag{A8}$$

for some constant coefficient η_k. Therefore, the time $\tau_k(x)$ for the front to advance to position x is equal to

$$\tau_k(x) = \frac{x^2}{4\eta_k^2 D}. \tag{A9}$$

Note that the partial differential equation, Eqn. 68, or its equivalent integrated form given by Eqn. A5 apply to the general case of combined advection and diffusion for arbitrary boundary conditions of concentration, flux, or some mixed form.

Quasi-Stationary State Approximation

The time evolution of a geochemical system can be expediently calculated over geologic time spans using the quasi-stationary state approximation (LICHTNER, 1988, 1991). In this approximation the partial time derivative of the solute concentration in Eqn. 4 is neglected compared to the remaining terms. This results in the ordinary differential equation

$$\frac{d}{dx}\left(\phi D \frac{dC_j^{(k)}}{dx}\right) - u\frac{dC_j^{(k)}}{dx} = \nu_{jm}\frac{\partial S_m^{(k)}}{\partial t}, \tag{A10}$$

in which the time t enters only as a parameter through the positions of the reaction zone boundaries. The evolution of the reaction zone boundaries with time is obtained by integrating the Rankine-Hugoniot equations given by Eqn. 10. These equations must be solved simultaneously with mineral mass transfer equations accounting for internal reaction within each alteration zone.

In order to carry out the integration of the Rankine-Hugoniot equations, it is necessary to know the initial jumps in the mineral modal abundances across each reaction front. The Rankine-Hugoniot equations themselves determine the mineral modal abundance on the upstream side of each reaction front in terms of the modal abundance of the mineral on the downstream side of the front which is not present on the upstream side. This is the case for zones AB_2 and AB for which $S_{AB_2}^{\langle 2-\rangle}$ and $S_{AB}^{\langle 3-\rangle}$ are determined by the Rankine-Hugoniot equations according to Eqns. A1 and A2. However, this still leaves the modal abundance of minerals on the upstream boundary of each reaction zone undetermined. These correspond to $S_{AB_2}^{\langle 1+\rangle}$ and $S_{AB}^{\langle 2+\rangle}$. To obtain these quantities it is necessary to integrate the mineral mass transfer equations given by Eqn. 68, accounting for internal reaction within each zone.

APPENDIX B

Pure Diffusive Transport

The first correct solution to the transport-reaction problem for diffusion with constant porosity for conditions local equilibrium was given only recently by NOVAK et al. (1989). BALASHOV and LEBEDEVA (1991) considered kinetic reactions and took into account changes in porosity as well. This appendix considers the general form of solutions to partial differential equations with the structure

$$\frac{\partial}{\partial t}(\phi C) = \frac{\partial}{\partial x}\left(D\phi \frac{\partial C}{\partial x}\right) + \frac{\partial S}{\partial t}. \tag{B1}$$

Equations of this form for a set of independent primary species augmented by algebraic equations representing mineral equilibria, describe transport by diffusion taking into account mineral precipitation and dissolution reactions represented by the function $S(x, t)$.

If the transformation

$$x' = ax, \tag{B2}$$

and

$$t' = a^2 t, \tag{B3}$$

is carried out on the diffusion-reaction equation for some real number a, it follows that the equation remains invariant under the transformation, that is

$$\frac{\partial}{\partial t'}(\phi C) = \frac{\partial}{\partial x'}\left(D\phi \frac{\partial C}{\partial x'}\right) + \frac{\partial S}{\partial t'}. \tag{B4}$$

Thus, provided the initial and boundary conditions are also invariant, the solutions to the transport equation must be the same. It follows that the concentration at position x' and time t' is equal to the concentration at position x and time t:

$$C(x', t') = C(x, t). \tag{B5}$$

Similar relations hold for the mineral concentration S and the porosity ϕ:

$$S(x', t') = S(x, t), \tag{B6}$$

and

$$\phi(x', t') = \phi(x, t). \tag{B7}$$

Furthermore, it follows that the pairs (x', t') and (x, t) are related by

$$\frac{x'}{\sqrt{t'}} = \frac{x}{\sqrt{t}}. \tag{B8}$$

This implies that solutions to the transport equation can be represented as a function of a single variable η, referred to as a similarity variable, defined by

$$\eta(x, t) = \frac{x}{2\sqrt{Dt}} = \frac{x'}{2\sqrt{Dt'}}, \tag{B9}$$

where the factor of 2 and the diffusion coefficient D are included for convenience. The proof given for the existence of a similarity variable, although limited to concentration boundary conditions, is otherwise very general and also applies to situations in which the porosity varies throughout the system.

In terms of the similarity variable η, the transport equation becomes

$$\frac{d}{d\eta}\left(\phi \frac{dC}{d\eta}\right) + 2\eta\frac{d}{d\eta}(\phi C) = \frac{dS}{d\eta}, \tag{B10}$$

and thus the transport problem is reduced to solving an ordinary differential equation in the similarity variable η. In the quasi-stationary state approximation these equations become

$$\nu_{jm}\frac{dS_m}{d\eta} = -\frac{\phi}{2\eta}\frac{d^2C_j}{d\eta^2}. \tag{B11}$$

The Rankine-Hugoniot equations reduce to the expression

$$\eta_k = -\frac{\phi}{2}\frac{[dC_j/d\eta]_k}{\sum_m \nu_{jm}[S_m]_k}, \tag{B12}$$

which no longer involves the derivative of the position of the reaction front with respect to time. The porosity is a function of the mineral volume fractions through a relation of the form

$$\phi(\eta) = 1 - \sum_m \bar{\phi}_m(\eta). \tag{B13}$$

This equation, however, does not take into account the possible creation of disconnected pore spaces that do not contribute to transport.

It is interesting to note that the existence of a similarity variable η implies that all quantities evaluated at zone boundaries must be constant in time. Differentiating the relation for the concentration

$$C(ax, a^2t) = C(x, t), \tag{B14}$$

with respect to the parameter a yields the partial differential equation

$$x\frac{\partial C}{\partial x} + 2t\frac{\partial C}{\partial t} = 0, \tag{B15}$$

after replacing a by unity. The velocity of a point $l(t)$ of constant concentration is given by the equation

$$\frac{dl}{dt} = -\frac{\partial C/\partial t}{\partial C/\partial x}. \tag{B16}$$

Using Eqn. B15 and replacing x with $l(t)$ the expression for the velocity becomes

$$\frac{dl}{dt} = \frac{l(t)}{2t}, \tag{B17}$$

which may be integrated to yield

$$l(t) = \text{constant} \times t^{1/2}. \tag{B18}$$

This equation has the same time dependence as obtained for the dependence of the reaction front positions on time from the definition of η by substituting $l_k(t)$ for x yielding the expression

$$l_k(t) = 2\eta_k\sqrt{Dt}, \tag{B19}$$

where η_k is a constant different for each front. Thus in η-space the zone boundaries are fixed at positions η_1, η_2, η_3. The solute concentrations and mineral volume fractions are constant at each boundary.

To evaluate the Rankine-Hugoniot equations, it is necessary to compute the jump in the concentration gradient across each reaction front. Within each monomineralic reaction zone there exists one conserved quantity that does not involve chemical reactions. By forming the appropriate linear combinations of Eqn. B11 one obtains for the kth reaction zone containing the mth mineral the conservation relation

$$\frac{d^2\chi_k}{d\eta^2} = 0, \tag{B20}$$

where

$$\chi_k = \nu_{Bm}C_A^{(k)} - \nu_{Am}C_B^{(k)}. \tag{B21}$$

Integrating this equation once yields

$$\frac{d\chi_k}{d\eta} = \frac{\Delta\chi_k}{\Delta\eta_k}, \tag{B22}$$

with

$$\Delta\chi_k = \chi_k^k - \chi_k^{k-1}, \tag{B23}$$

and

$$\Delta\eta_k = \eta_k - \eta_{k-1}. \tag{B24}$$

A further integration yields the result

$$\chi_k(\eta) = \frac{\eta - \eta_{k-1}}{\Delta\eta_k}\Delta\chi_k + \chi_k^{k-1}, \tag{B25}$$

resulting in a linear variation of χ_k with η characteristic of transport by diffusion. An equal number of equations as unknowns are obtained by writing Eqn. B22 in the form

$$\nu_{Bm}\frac{dC_A^{(k)}}{d\eta} - \nu_{Am}\frac{dC_B^{(k)}}{d\eta} = \frac{\Delta\chi_k}{\Delta\eta_k}, \tag{B26}$$

combined with derivatives of the mass action equations

$$\nu_{Am}\frac{1}{C_A^{(k)}}\frac{dC_A^{(k)}}{d\eta} + \nu_{Bm}\frac{1}{C_B^{(k)}}\frac{dC_B^{(k)}}{d\eta} = 0. \tag{B27}$$

Mineral modal abundances at opposite ends of a reaction zone are related by the equation

$$S_m^{\langle(k-1)+\rangle} = S_m^{\langle k-\rangle} + \frac{\phi}{2\nu_{jm}}\int_{\eta_{k-1}}^{\eta_k}\frac{1}{\eta}\frac{d^2C_j^{(k)}}{d\eta^2}\,d\eta, \tag{B28}$$

obtained by integrating Eqn. B11. The variation of the mineral modal abundance within the kth reaction zone is given by

$$S_m^{(k)}(\eta) = S_m^{\langle k-\rangle} + \frac{\phi}{2\nu_{jm}}\int_{\eta}^{\eta_k}\frac{1}{\eta}\frac{d^2C_j^{(k)}}{d\eta^2}\,d\eta. \tag{B29}$$

In order for an acceptable solution to exist, it is necessary that the quantities η_k satisfy the inequality

$$\eta_1 \le \eta_2 \le \eta_3, \tag{B30}$$

similar to Eqn. 29 for pure advective transport. In addition the mineral modal abundances and solute concentrations must be positive.

Referring to Fig. 3, the short dashed line dividing the field labeled II represents the condition $\eta_1 = \eta_2$, giving the threshold condition for zone AB_2 to be absent in the alteration column. Above this curve the sequence $\mathcal{F}|AB_2|AB|A_2B$ is obtained, whereas below the curve the sequence $\mathcal{F}|AB|A_2B$ occurs.

APPENDIX C

Internal Reaction Rates

This appendix derives expressions for the internal rate of reaction in zones AB_2 and AB. Within reaction zone AB, the solute concentration satisfies the differential equations

$$\hat{L}C_A = -\mathcal{I}_{AB}, \tag{C1}$$

and

$$\hat{L}C_B = -\mathcal{I}_{AB}, \tag{C2}$$

where $\hat{L}$ denotes the differential operator

$$\hat{L} = \frac{\partial}{\partial t}\phi - \frac{\partial}{\partial x}\left(\phi D\frac{\partial}{\partial x}\right) + u\frac{\partial}{\partial x}. \tag{C3}$$

Subtracting these equations leads to the conservation equation

$$\hat{L}[C_A - C_B] = 0. \tag{C4}$$

The relation Eqn. C4 implies that the quantity in square brackets is conserved (LICHTNER, 1991). Denoting this quantity by χ_{AB} the solute concentration within zone AB can be determined in terms of the function χ_{AB} by solving the following two equations simultaneously:

$$C_A - C_B = \chi_{AB}, \tag{C5}$$

and

$$C_AC_B = K_{AB}^{-1}. \tag{C6}$$

These equations have the explicit solution

$$C_A = (\chi_{AB} + [\chi_{AB}^2 + 4K_{AB}^{-1}]^{1/2})/2, \tag{C7}$$

and

$$C_B = (-\chi_{AB} + [\chi_{AB}^2 + 4K_{AB}^{-1}]^{1/2})/2. \tag{C8}$$

By differentiating Eqns. C5 and C6 implicitly yields the following expressions for the derivatives of C_A and C_B in terms of the derivative of χ_{AB}:

$$\frac{\partial C_A}{\partial x} = \frac{C_A}{C_A + C_B}\frac{\partial\chi_{AB}}{\partial x}, \tag{C9}$$

and

$$\frac{\partial C_B}{\partial x} = -\frac{C_B}{C_A + C_B}\frac{\partial \chi_{AB}}{\partial x}, \qquad \text{(C10)}$$

Substituting these results into Eqn. A2 and noting the derivative of χ_{AB} cancels yields Eqn. A3.

Similar results can be derived for the reaction zone containing mineral AB_2. In this case the solute concentration satisfies the differential equations

$$\hat{\mathcal{L}} C_A = -\mathcal{I}_{AB_2}, \qquad \text{(C11)}$$

and

$$\hat{\mathcal{L}} C_B = -2\mathcal{I}_{AB_2}. \qquad \text{(C12)}$$

Eliminating the reaction rate I leads to the equation

$$\hat{\mathcal{L}}[2C_A - C_B] = 0. \qquad \text{(C13)}$$

Denoting the quantity in brackets by χ_{AB_2}, the solute concentration within zone AB_2 can be determined in terms of the function χ_{AB_2} by solving the following two equations simultaneously:

$$2C_A - C_B = \chi_{AB_2}, \qquad \text{(C14)}$$

and

$$C_A C_B^2 = K_{AB_2}^{-1}. \qquad \text{(C15)}$$

These equations lead to a cubic equation in C_A or C_B which may be solved analytically. The resulting expression, however, is too long to present here. Alternatively a numerical solution can also be easily found. By differentiating Eqns. C14 and C15 implicitly with respect to x yields the following expressions for the first derivative of C_A and C_B in terms of the derivative of χ_{AB_2}:

$$\frac{\partial C_A}{\partial x} = \frac{2C_A}{4C_A + C_B}\frac{\partial \chi_{AB_2}}{\partial x}, \qquad \text{(C16)}$$

and

$$\frac{\partial C_B}{\partial x} = -\frac{C_B}{4C_A + C_B}\frac{\partial \chi_{AB_2}}{\partial x}. \qquad \text{(C17)}$$

To derive expressions for the internal reaction rate in zones AB and AB_2 note that the operator $\hat{\mathcal{L}}$ applied to the product of two functions f and g yields

$$\hat{\mathcal{L}}[fg] = \hat{\mathcal{L}}[f]g + f\hat{\mathcal{L}}[g] - 2\phi D\frac{\partial f}{\partial x}\frac{\partial g}{\partial x}. \qquad \text{(C18)}$$

For zone AB take $f = C_A$ and $g = C_B$ which yields

$$\mathcal{I}_{AB} = -2\phi D\frac{1}{C_A + C_B}\frac{\partial C_A}{\partial x}\frac{\partial C_B}{\partial x}, \qquad \text{(C19)}$$

making use of Eqns. C1, C2, and C6. Substituting Eqns. C9 and C10 yields

$$\mathcal{I}_{AB} = 2\phi D\frac{C_A C_B}{(C_A + C_B)^3}\left(\frac{\partial \chi_{AB}}{\partial x}\right)^2. \qquad \text{(C20)}$$

For zone AB_2, take $f = C_A$ and $g = C_B^2$. This yields the result

$$\hat{\mathcal{L}}[C_A C_B^2] = \hat{\mathcal{L}}[C_A]C_B^2 + C_A\hat{\mathcal{L}}[C_B^2] - 4\phi D C_B\frac{\partial C_A}{\partial x}\frac{\partial C_B}{\partial x}. \qquad \text{(C21)}$$

Applying Eqn. C18 to the term $\hat{\mathcal{L}}[C_B^2]$ taking $f = g = C_B$ yields

$$\hat{\mathcal{L}}[C_B^2] = 2C_B\hat{\mathcal{L}}[C_B] - 2\phi D C_B\left(\frac{\partial C_B}{\partial x}\right)^2. \qquad \text{(C22)}$$

Combining these relations yields the result

$$\mathcal{I}_{AB_2} = -2\phi D\frac{1}{(4C_A + C_B)C_B}\left\{2C_B\frac{\partial C_A}{\partial x} + C_A\frac{\partial C_B}{\partial x}\right\}\frac{\partial C_B}{\partial x}. \qquad \text{(C23)}$$

Substituting Eqns. C16 and C17 for the partial derivatives yields the expression

$$\mathcal{I}_{AB_2} = 6\phi D\frac{C_A C_B}{(4C_A + C_B)^3}\left(\frac{\partial \chi_{AB_2}}{\partial x}\right)^2. \qquad \text{(C24)}$$

Equations C20 and C24 may be further evaluated using explicit expressions for χ_{AB} and χ_{AB_2}.